NASA/CR—2008-215237

Intelligent Engine Systems

Alternate Fuels Evaluation

Dilip Ballal
The University of Dayton, Dayton, Ohio

June 2008

NASA STI Program . . . in Profile

Since its founding, NASA has been dedicated to the advancement of aeronautics and space science. The NASA Scientific and Technical Information (STI) program plays a key part in helping NASA maintain this important role.

The NASA STI Program operates under the auspices of the Agency Chief Information Officer. It collects, organizes, provides for archiving, and disseminates NASA's STI. The NASA STI program provides access to the NASA Aeronautics and Space Database and its public interface, the NASA Technical Reports Server, thus providing one of the largest collections of aeronautical and space science STI in the world. Results are published in both non-NASA channels and by NASA in the NASA STI Report Series, which includes the following report types:

- TECHNICAL PUBLICATION. Reports of completed research or a major significant phase of research that present the results of NASA programs and include extensive data or theoretical analysis. Includes compilations of significant scientific and technical data and information deemed to be of continuing reference value. NASA counterpart of peer-reviewed formal professional papers but has less stringent limitations on manuscript length and extent of graphic presentations.

- TECHNICAL MEMORANDUM. Scientific and technical findings that are preliminary or of specialized interest, e.g., quick release reports, working papers, and bibliographies that contain minimal annotation. Does not contain extensive analysis.

- CONTRACTOR REPORT. Scientific and technical findings by NASA-sponsored contractors and grantees.

- CONFERENCE PUBLICATION. Collected papers from scientific and technical conferences, symposia, seminars, or other meetings sponsored or cosponsored by NASA.

- SPECIAL PUBLICATION. Scientific, technical, or historical information from NASA programs, projects, and missions, often concerned with subjects having substantial public interest.

- TECHNICAL TRANSLATION. English-language translations of foreign scientific and technical material pertinent to NASA's mission.

Specialized services also include creating custom thesauri, building customized databases, organizing and publishing research results.

For more information about the NASA STI program, see the following:

- Access the NASA STI program home page at *http://www.sti.nasa.gov*

- E-mail your question via the Internet to *help@sti.nasa.gov*

- Fax your question to the NASA STI Help Desk at 301–621–0134

- Telephone the NASA STI Help Desk at 301–621–0390

- Write to:
  NASA Center for AeroSpace Information (CASI)
  7115 Standard Drive
  Hanover, MD 21076–1320

NASA/CR—2008-215237

Intelligent Engine Systems

Alternate Fuels Evaluation

Dilip Ballal
The University of Dayton, Dayton, Ohio

Prepared under Contract NAS3–01135, Work element 5, Task order 37

National Aeronautics and
Space Administration

Glenn Research Center
Cleveland, Ohio 44135

June 2008

This work was sponsored by the Fundamental Aeronautics Program at the NASA Glenn Research Center.

Level of Review: This material has been technically reviewed by NASA technical management.

Available from

NASA Center for Aerospace Information
7115 Standard Drive
Hanover, MD 21076–1320

National Technical Information Service
5285 Port Royal Road
Springfield, VA 22161

Available electronically at http://gltrs.grc.nasa.gov

Table of Contents

Intelligent Engine Systems
Alternate Fuels Evaluation

Dilip Ballal
The University of Dayton
Dayton, Ohio 45469

Program Objectives
The University of Dayton performed work on the following subtasks.

- Subtask 5.2.1: High temperature shock tube measurements
- Subtask 5.2.2: Chemical kinetic analysis of representative fuel mixtures
- Subtask 5.2.3: Well Stirred Reactor (WSR) tests

These data sets and chemical kinetic analysis were used in the interpretation of data. Now, it will be possible to formulate detailed chemical kinetics models of ignition, lean blowout, combustion performance, and emissions from alternative fuels of the future.

Subtask 5.2.1: High Temperature Shock Tube Measurements
Shock tubes are well suited to study ignition delays of fuel-air mixtures at very high pressure and temperatures that are representative of the operating environment of a modern gas turbine combustor. Also, chemistry of soot particulate formation can be studied. A main advantage of the shock tube is that parameters like temperature, pressure, fuel concentration, and stoichiometry can be changed independently. Our shock tube facility was developed under a previous NASA Propulsion 21 funding (modification 2 of Work Element 2.1) and is fully described by Sidhu et al. (2005).

As shown in Figure 1, it consists of a 21 feet long high-pressure single pulse reflected shock tube capable of short duration exposures (~0.1-8 ms) at very high temperatures (~3000°C) and pressures (~50 atm.). Real-time sensors provide information related to the shock velocity, pressure, and temperature as well as the timing of combustion events such as ignition delay and burnout. Post-run sampling can be performed and properties of the collected samples are typically analyzed by reflectance spectroscopy, thermal desorption, carbon burn off analysis and high-resolution GC/FID/MS, GC/MS-MS, or multidimensional GC/MS-MS.

Figure 1: The UDRI high pressure, single pulse, reflected shock tube as viewed from the driver section.

The objective of this task was to investigate ignition characteristics of surrogate synthetic jet fuels. One of the main characteristic features of the Fischer-Tropsch synthetic fuel is their significantly higher concentration of methylated alkanes (C_8-C_{16}) when compared to kerosene based jet fuels like Jet-A and JP-8. For this reason we chose 2-methyl heptane (C_8) with an adequate vapor pressure (22 torr at 760 mmHg), to be a surrogate synthetic jet fuel for this study. All experiments were conducted under premixed combustion condition. Before each experiment the test section was filled with argon and then 2-methyl heptane (in Argon) and oxygen were metered in to obtain a pre-determined fuel/air ratio. Experiments were conducted over a temperature range of 1100 K – 1700 K at pressures of 20 to 48 atm, and equivalence ratios of 0.5, 3.0 and 4.0.

The gas used in the driver section was predominantly helium with some argon added to help achieve the required longer dwell times. The dwell time, for this proposed study were on the order of ~7.5 ms. For all experiments, the nominal test conditions were set by the initial state of the system and the actual test conditions were determined from the reflected shock velocity through the test gas. The high pressure, high temperature shock heated gas behind the reflected shock provides the fuels an exposure similar to that experienced in an engine combustion chamber. To determine the actual test conditions, the incident velocity was measured by dividing the distance by the arrival time of the shock past two piezoelectric pressure transducers mounted on the sidewall and end plate. The conditions in the test section were then calculated using the shock solution model of CHEMKIN 4.0 for which the mechanism and thermodynamic data for the reacting species was obtained from the National Institute of Standards (NIST) data base.

All pressure events were monitored using a single-sweep digital oscilloscope with two channels indicating events related to the pressure pulses generated from the pressure transducer mounted on the sidewall and endplate of the test section and a third indicating combustion monitored with a silicon optical pressure sensor (responsivity of 190-1100 nm) that detects the radiation emitted during combustion. The ignition delay times were determined with the optical sensor data and the data from the pressure transducer at the end plate. The fire control system closes the pneumatic test section isolation valve approximately 0.5 s after the diaphragm that separates the driver and the driven section is ruptured, sealing the combustion products in the test section. After each test, the exhaust valve to the sampler was opened and the test section was purged with ~25 L (~10 change volumes) of dry helium immediately after the isolation valve closed. This ensures that combustion gases are removed from the system and are captured in a 25 L Tedlar sample bag to be used later for fixed, volatile and semi-volatile product analyses. The ignition delay and product distribution data collected in this study will be very useful in developing an ignition model, database on low-residence time chemical kinetics, and formation of intermediate radicals and species for pollutant emissions studies. Such studies will help refine models of ignition and turbulent combustion used to design the current ultra-high pressure, ultra-fuel lean advanced gas turbine combustors such as TAPS (see Sidhu et al. 2005) and also future designs.

Ignition Delay

Gas turbine combustors of the future are operating at higher and higher pressure and will be soon approaching operating pressures of 50 atm. In the lean-premixed combustors, autoignition and flame flashback must be avoided at all costs because it could damage combustor and turbine components. Therefore, an understanding of the ignition delay time is essential. For this study, ignition delay times of 2-methyl heptane

were measured over a temperature range of 1100 to 1700 K at pressures of 20 to 48 atm., and Φ = 0.5, 3.0 and 4.0. These results are shown in Table 1.

Table1. Ignition delay times for 2-methyl heptane

Phi	Ignition Delay	P5	T5
	(μsec)	(atm)	(K)
0.5	176	44.1	1658
0.5	191	44.28	1635
0.5	182	44.41	1582
0.5	192	44.89	1541
0.5	208	45.14	1521
0.5	289	45.6	1465
0.5	301	47.62	1483
0.5	503	43.57	1386
0.5	454	47.37	1420
Phi	**Ignition Delay**	**P5**	**T5**
	(μsec)	**(atm)**	**(K)**
3	4200	23.632	1128
3	2570	22.879	1138.8
3	2260	23.875	1144.2
3	2400	23.651	1145.3
3	2131	22.324	1148.5
3	2221	21.553	1156.4
3	2114	23.711	1163.7
3	1900	22.763	1163.7
3	1884	21.383	1208.2
3	1971	22.808	1208.2
3	1710	23.202	1209.3
3	1710	22.932	1222.3
3	1665	22.523	1222.3
3	1620	22.071	1225.2
3	1660	21.488	1243.4
3	1542	21.569	1245.9
3	1340	21.632	1251.5
3	1400	19.873	1258
3	1410	21.097	1269.3
3	1360	21.923	1270.2
3	1422	21.471	1270.2
3	1330	21.273	1271.4
3	1200	21.702	1274.5
3	1040	21.006	1296.5
3	1230	20.815	1297.6
3	1020	21.14	1304.8
3	896	20.867	1333
3	888	20.678	1334.1
3	848	20.996	1341.4
3	628	20.659	1372.9

3	501	20.072	1402.6
3	425	20.326	1416.6
3	406	19.863	1445.4
3	422	19.619	1459
3	368	20.106	1459.6
3	408	19.565	1473.4
3	328	19.769	1473.9
3	349	19.929	1493.3
3	339	19.312	1496.6
3	306	19.65	1507.2
3	312	19.564	1526.2
3	340	19.752	1534.7
3	342	19.791	1540.9
3	298	19.233	1554.5
3	302	19.659	1574.4
3	1901	20	1220
Phi	**Ignition Delay**	**P5**	**T5**
	(μsec)	**(atm)**	**(K)**
4	1719	20.396	1246.4
4	1360	20.814	1297.6
4	1120	19.947	1308
4	1090	18.979	1315.8
4	920	19.777	1395.1
4	1010	19.881	1349.9
4	593	19.885	1454.7
4	480	19.334	1493.3
4	404	19.149	1555

Subtask 5.2.2: Chemical kinetic analysis of representative fuel mixtures
The experiments at higher equivalence ratios (3 and 4) had to be conducted at lower pressures (20 atm) to avoid experimental problems caused by high soot yields at higher pressures (45-50 atm). The ignition delay data collected at different pressures was compared after it had been normalized using equation 1 below.

$$T_{ign} \propto P_5 \, \alpha \exp (E_A/R\,T) \qquad (1)$$

After normalization, the ignition delay data for all three equivalence ratios falls into three straight lines on a semi-log graph (see Figure 2). The activation energy for 2-methyl heptane ignition is approximately 21 Kcal/mole based on the slopes of three lines in Figure 2. This activation energy is 20 Kcal/mole less than the activation energy calculated by Davidson et al. (1999) for n-heptane ignition. The activation energy of 2-methyl heptane is also 13 Kcal/mole less the n-heptane ignition activation energy that we calculated previously from our 50 atm heptane ignition study (see Figure 3).

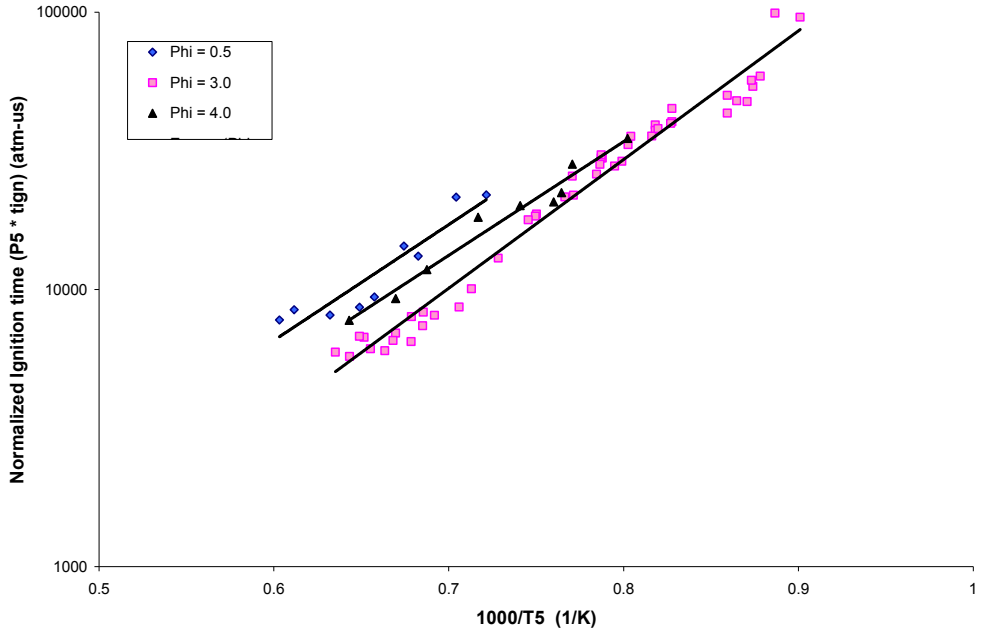

Figure 2. Ignition delay times for 2-methyl heptane ignition at Φ=0.5, 3, and 4.0.

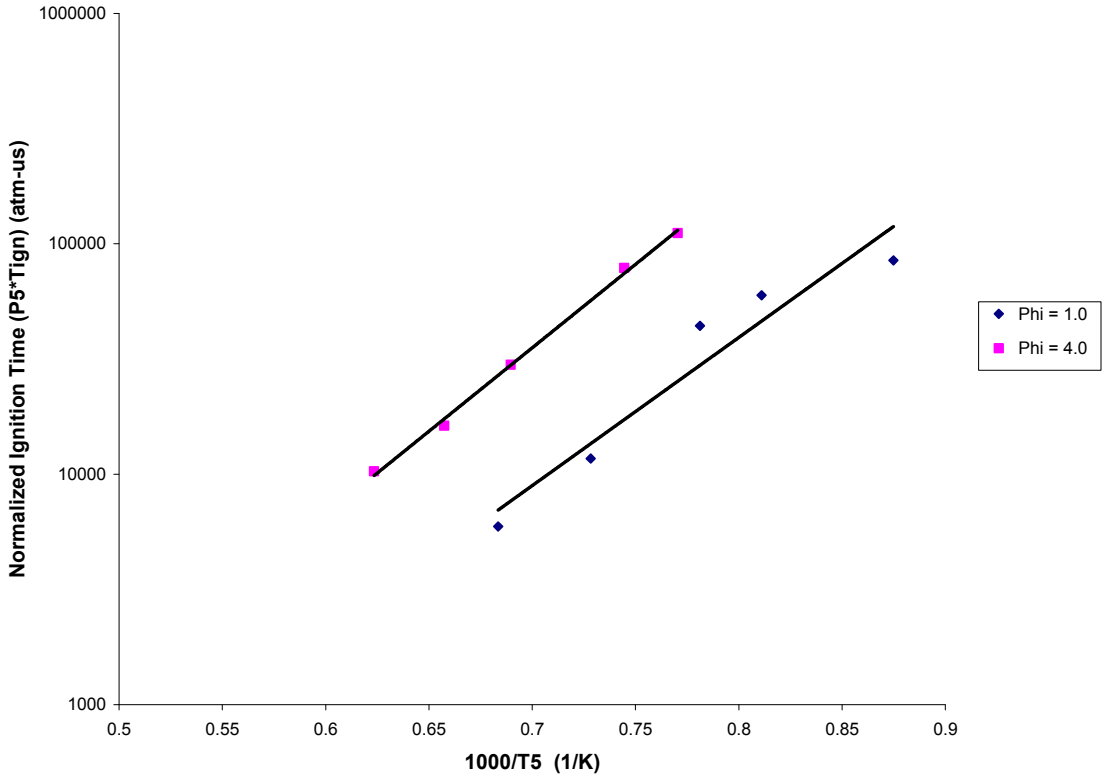

Figure 3. Ignition delay times for n-heptane ignition at Φ= 1.0 and 4.0.

Subtask 5.2.3: Well Stirred Reactor (WSR) Tests

WSR is a versatile laboratory research combustor that simulates the highly turbulent combustion process in a practical gas turbine combustor. Figure 4 shows a photograph of the atmospheric pressure WSR. Stouffer et al. (2005) have described the development & combustion performance of this WSR.

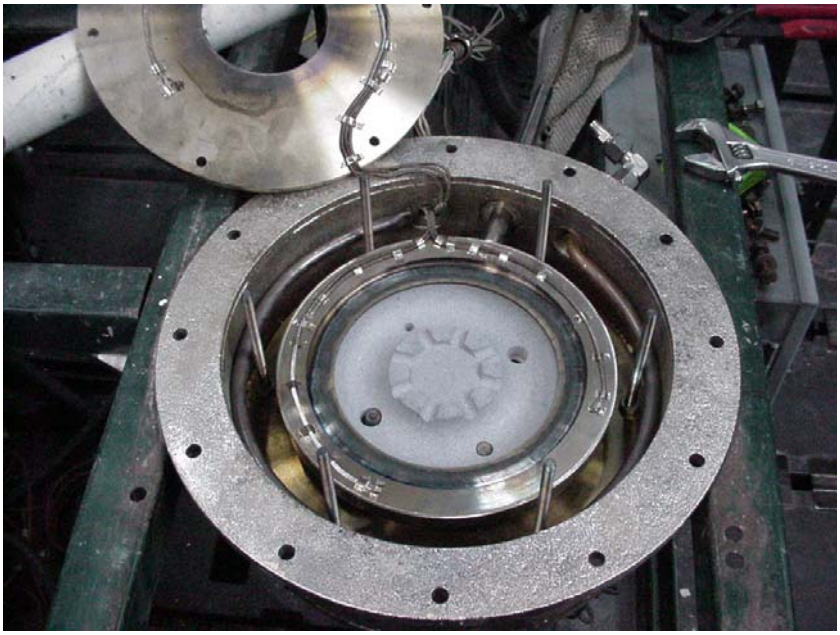

Figure 4: WSR for atmospheric pressure

Interest in alternative fuels has led to the consideration of the Fischer-Tropsch (FT) process for converting non-conventional hydrocarbon feedstock into a practical gas turbine fuel. The FT process allows the use of non-conventional hydrocarbons by converting the fuel into synthesis gas (CO and H_2), which can then be converted to hydrocarbon fuel sources. The raw feedstock fuel for the process can be natural gas, coal or other sources. The Department of Defense is currently working with the Department of Energy to develop, test, and certify usage of the FT fuels leading to their use in military and commercial aircraft. The performance and emissions characteristics were measured for the Well-Stirred Reactor WSR operating for two fuels: JP8 and a synthetic Fisher-Tropsch fuel (S8) over both lean and rich equivalence ratios.

The properties for the two fuels are shown in Table 2. JP8 is the standard fuel used in U.S. military aircraft. Syntroleum Corporation of Tulsa, OK, produced the S8 fuel from a feedstock of natural gas. However, because the initial step in the fuel manufacturing is to produce synthesis gas, which is then converted to the jet fuel, the properties of the FT fuel considered here are similar to those that would be made by the FT process using other feedstock, such as coal. The FT fuel is primarily composed of normal and branched alkanes, in contrast to JP8, which can have significant (10-24%) aromatic content. As shown in Table 1 many of the properties of the S8 are similar to those for JP8.

Our first set of results was published as an AIAA Paper 2007-5673 attached as Appendix A. Further work was performed after writing this paper as follows.

Table 2: Properties of the JP8 and FT Fuels

Property	JP8 (3773)	FT (5018)
Molecular Formula	$C_{11.9}H_{22.8}$	$C_{11.9}H_{25.9}$
H/C ratio	1.916	2.165
Stoichiometric Fuel/air	0.0682	0.0666
Molecular Weight	165.9	169.5
Density (g/ml)	0.80	0.755
Heat of Combustion (J/kg)	43276	44135
% Aromatics	17.2	0
Freezing Point (°C)	-51	-51
Flash Point (°C)	45	48

Lean Blowout and Emissions Experiments

The performance and gaseous emissions were measured for the Well-Stirred Reactor WSR operating under lean conditions for two fuels: JP8 and a synthetic Fisher-Tropsch fuel (S8) over a range of equivalence ratios from 0.6 down to the lean blowout limits. The tests were conducted at a range of air flow rates from 300 to 600 g/min, which corresponds to a range of residence times from 5-12 ms at the combustion temperatures in the reactor. Because of the emphasis on lean blowout studies the reactor was fitted with fused silica ceramics to minimize heat loss. The lean blowout characteristics were determined in LBO experiments at loading parameter values from 0.7 to 1.4. The lean blowout characteristics were then explored under higher loading conditions by simulating higher altitude operation with the use of nitrogen as a dilution gas for the air stream.

One of the primary measures of combustor performance in the WSR is the temperature in the combustor. Figure 5 shows the temperatures measured in the WSR in the lean range. The temperatures show close agreement for both fuels at the two flow rates. The temperature results are also compared to equilibrium calculations of the adiabatic flame temperature from the NASA Chemical Equilibrium Code. The difference between the experimental temperatures and the calculated adiabatic flame temperature were highest for the lower flow rate conditions implying that the effect of heat loss was less for the higher flow rate cases.

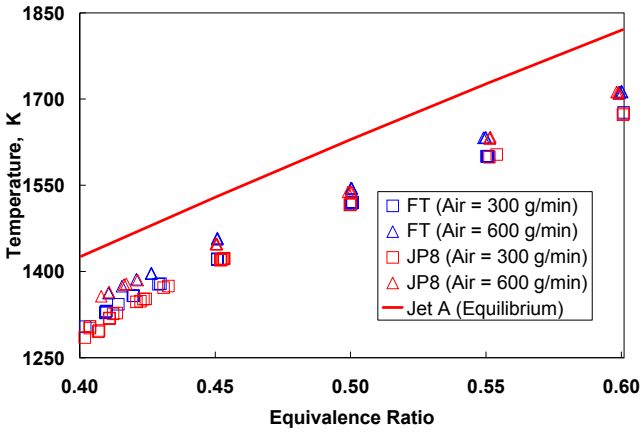

Figure 5. Comparison of combustion temperatures for FT and JP8 fuels in WSR.

The measured O_2 and CO_2 data are shown plotted along with the equilibrium values for JP8 and the ideal concentration for the FT fuel in Figures. 6 and 7, respectively. The overall results show the expected increased oxygen consumption and CO_2 production as the equivalence ratio is increased. It was found that with both of the fuels the CO_2 production was higher and the O_2 consumption was higher at the higher mass flow cases. This result is also consistent with trends of temperature vs. mass flow observed in Figure 5. The CO_2 observed for the JP8 was higher than that for the FT fuel, which was expected based on the higher carbon fraction for the JP8 fuel. For Φ >0.5 the ratio of the CO_2 produced for the JP8 to that for the FT ranged from 1.033-1.044, while the ideal ratio of the CO_2 produced under complete oxidation to CO_2 and H_2O for the two fuels was 1.044. For the higher equivalence ratios shown the results parallel the ideal limits, but as lean blowout was approached the oxygen consumption and CO_2 production depart further from the ideal limits. The departure from the ideal as lean blowout is approached is also consistent with the temperature trends shown above; as less CO_2 is formed the combustion temperatures decrease.

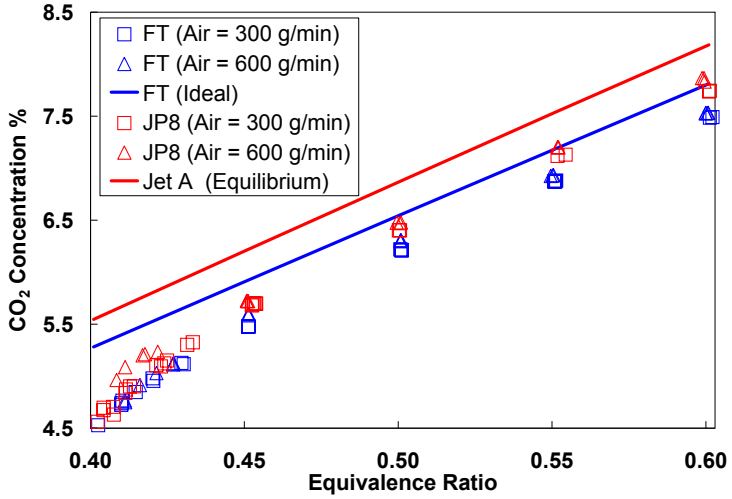

Figure 6. CO_2 concentration for FT and JP8 fuels in WSR.

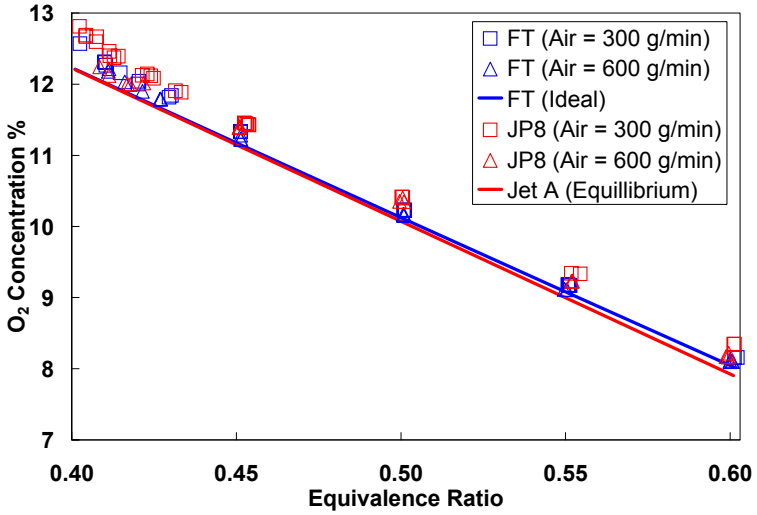

Figure 7: Oxygen concentration measured in the WSR

The water produced in the WSR was measured by an FTIR. The results are shown in Figure 8 along with an equilibrium and ideal calculation for the water in the exhaust based on complete conversion of the fuel to CO_2 and H_2O. The results show the expected increase in H_2O concentration with equivalence ratio and show good agreement with the equilibrium and ideal water concentrations. Because of the higher H/C ratio of the FT fuel, it was expected that the H_2O concentration in the exhaust would be higher for the FT than that for the JP8 fuel. A comparison of the experimental values in the range from Φ = 0.45 to 0.6 showed that the ratio of the water concentration for the FT exhaust to that of the JP8 was 1.07-1.09, which brackets the value of the ideal ratio (1.08) of the water produced for complete combustion of the two fuels.

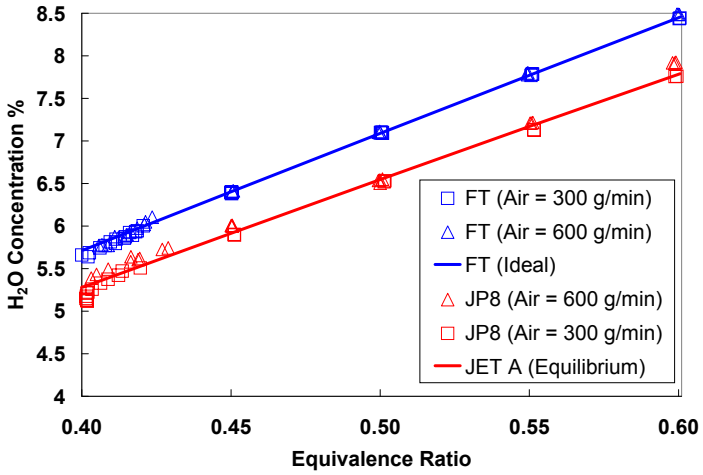

Figure 8. H_2O concentration measured in the WSR.

The NO concentration is shown in Figure 9 for the two fuels. Overall the levels for NO were low for both fuels as a result of the low temperatures. For the same flow rates little difference was seen between the two fuels.

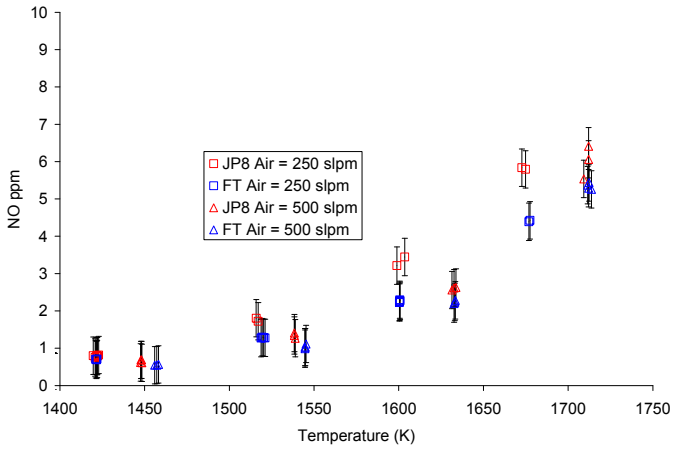

Figure 9. NO concentration for JP8 and FT fuels in the WSR (Φ = 0.4-0.6)

The combustion efficiency was calculated from the SAE Aerospace recommended Practice ARP 1533 using measurements of CO and UHC:

$$\eta_C = 1 - 10109\frac{EI_{CO}}{LHV} - \frac{EI_{UHC}}{1000} \quad (2)$$

where; EI is emissions index and LHV is the lower heating value of the fuel. The results (Figure 10) show that the combustion efficiency is almost identical for the two fuels. For equivalence ratio values above Φ = 0.5 the combustion efficiency was higher than 99% for both of the fuels. The major portion of the combustion inefficiency was due to the production of CO rather that the production of UHC's the lean blowout is approached at the lower equivalence ratios the combustion efficiency drops dramatically. The efficiency decrease with temperature drop is more pronounced for the shorter residence time cases.

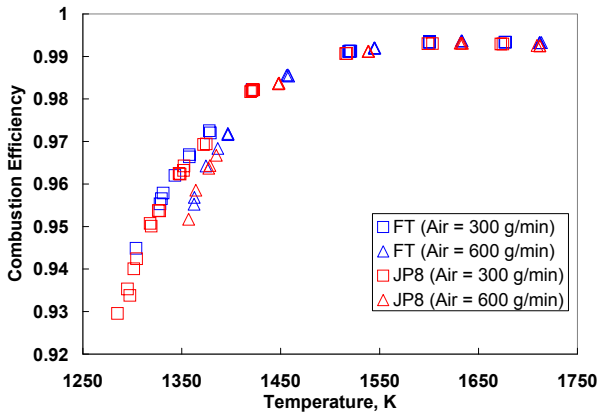

Figure 10. Combustion efficiency for FT and JP8 fuels for the WSR.

The response of the reactor to the lean blowout was also examined Figure 11 shows the lean blowout (LBO) data expressed as equivalence ratio at LBO vs. Loading parameter, LP, where the loading parameter is determined from:

$$LP = \frac{n_{air}}{VP^{1.75}} \quad (3)$$

where n_{air} = flow rate of air in moles/sec, V= volume of the reactor in liters, and P = pressure in the reactor in atm.

The LBO data for the JP8 show that the equivalence ratio at blowout varied only about 1% as the LP was doubled. This variation is actually less than the uncertainty of the measurement of the equivalence ratio. The data for the FT fuel show that the equivalence ratio at lean blowout is slightly less than that for the JP8 fuel and shows less than 2.8% increase in equivalence ratio with loading parameter as loading parameter is doubled.

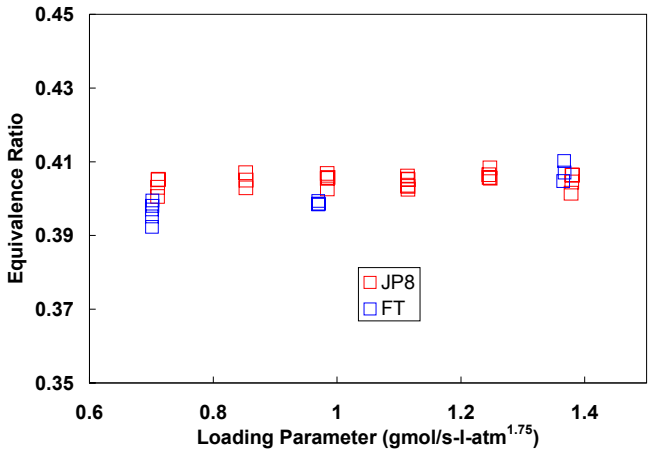

Figure 11. Equivalence ratio at lean blowout vs. air loading parameter.

The results of these experiments are summarized in further detail in an AIAA paper attached as Appendix A.

Rich Combustion Studies with Fischer-Tropsch and JP8 Fuels

A study was conducted on the emission characteristics and combustion performance for the two fuels in rich combustion. The range of equivalence ratios studied for the two fuels was from 1.85 up to the rich blowout limit of the fuels. The lower limit of equivalence ratio was imposed by the temperature limits of the ceramic used and was slightly above the soot inception limit for the two fuels. The air flow rate was maintained at a constant 300 g/min which corresponds to a range of residence times from 7.4-8.6 ms for the temperature range. A single blowout point was measured for both of the fuels and the blowout limits for the two fuels were found to be almost the same (Φ = 2.18 for JP8 and Φ = 2.2 for FT).

The temperature measurements for the two fuels are shown in Figure 12. As was it was for the lean combustion experiments, over moist of the range of equivalence ratios, the temperatures showed little difference (less than 20K) for the two fuels. The gaseous emissions for the major gaseous species are shown in Figures 13 to 16. The overall trends for the major species were as expected for a rich premixed, well-stirred reactor. Specifically, the oxygen level and unburned hydrocarbons increased along with the equivalence ratio while the carbon dioxide decreased. At each equivalence ratio the major species concentrations were similar. The O_2 and UHC were higher for the JP8 than for the FT fuels, however it should be noted that that blow out occurred at slightly lower levels for the JP8.

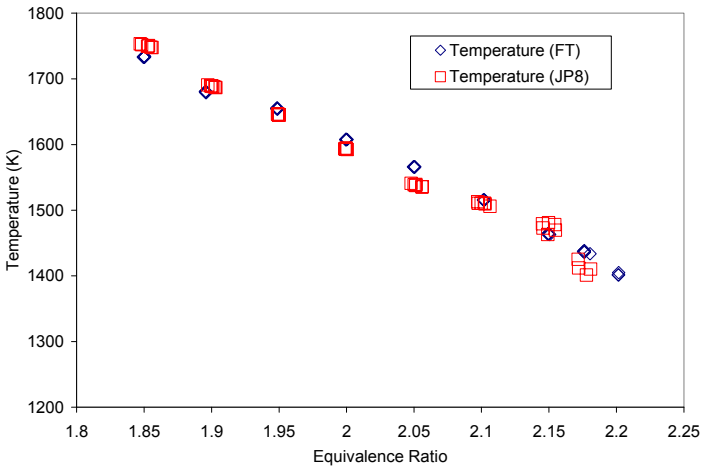

Figure 12. Measured temperatures during rich combustion with FT and JP8 fuels.

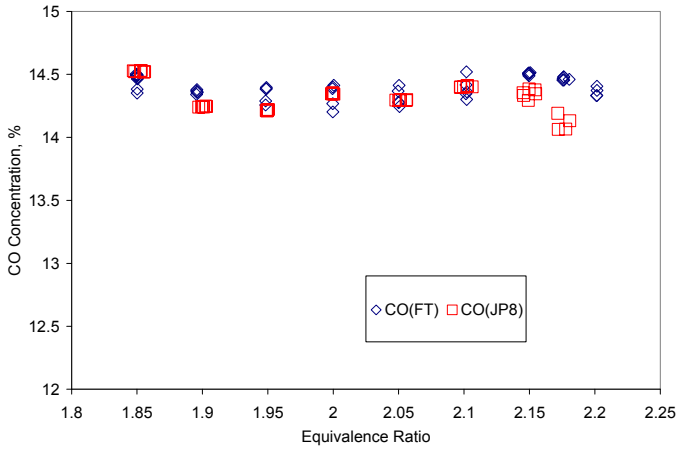

Figure 13. CO concentration in the WSR for FT and JP8 fuels.

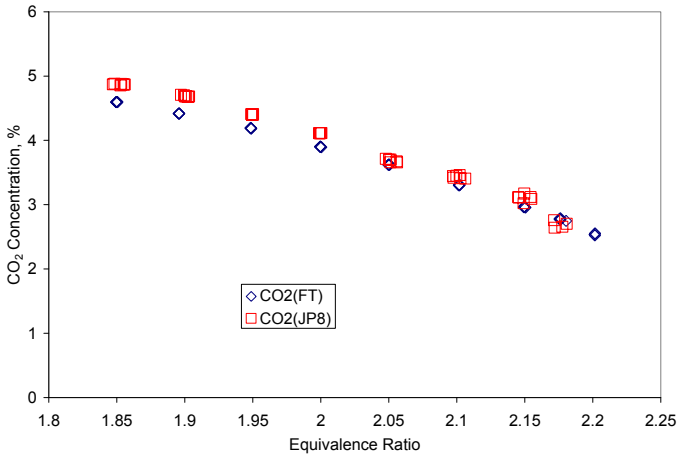

Figure 14. CO_2 concentration in the WSR for FT and JP8 fuels

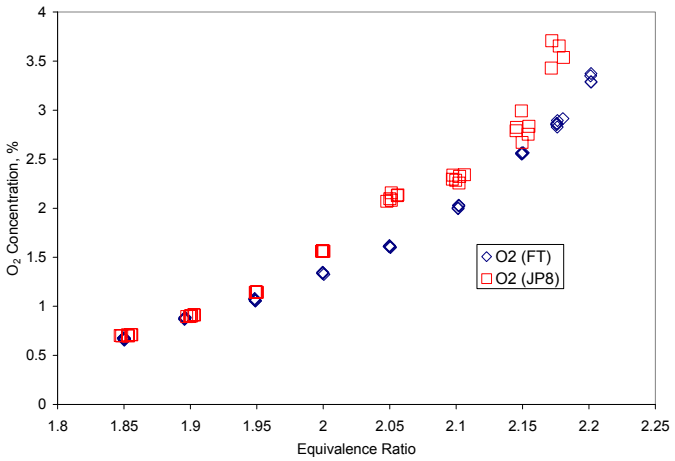

Figure 15. O_2 concentration in the WSR for FT and JP8 fuels

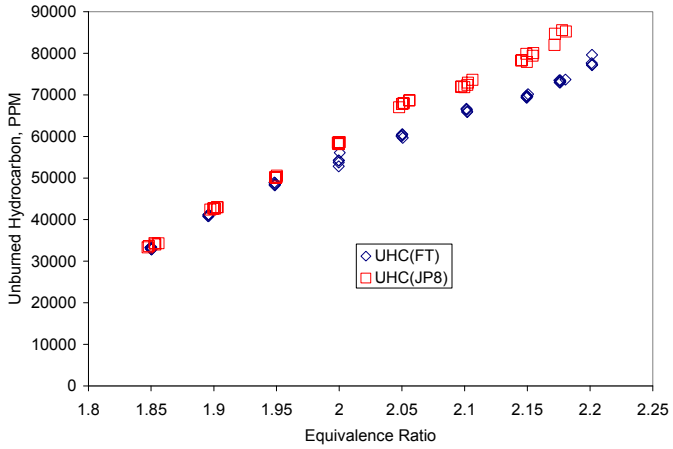

Figure 16. Unburned hydrocarbon concentration in the WSR for FT and JP8 fuels.

While the combustion temperatures and major species concentrations were similar for the two fuels, major differences were seen in the sooting characteristics of the two fuels. It was thought that the sooting characteristics of the two fuels would be dramatically different because of the high aromatic content of the JP8 fuel compared to the almost zero aromatic content of the FT fuels. During the experiment soot aerosol samples were extracted through quartz filters and the filters were analyzed by using a LECO apparatus to perform Temperature Programmed Oxidation (TPO) to determine the total carbon mass deposited on the filters. The results shown Figure 17, clearly demonstrate that the soot emissions for the JP8 fuel were 6-12 times higher than those for the FT fuel at the same equivalence ratio. Figure 18 shows photos for the same set of conditions. The filters for the JP8 experiments were clearly much darker than those for the FT experiment at the same equivalence ratios, which is in agreement with the quantitative results for carbon mass. In addition, the filters for the FT fuel exhibited a range of colors from light cream though brown which is more indicative of volatile incipient soot as compared to the much blacker more carbonaceous JP8 soot.

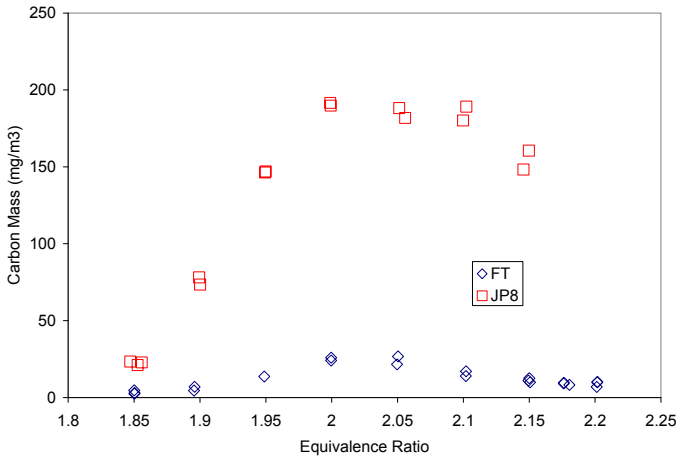

Figure 17. Total carbon mass measured in WSR for JP8 and FT fuels

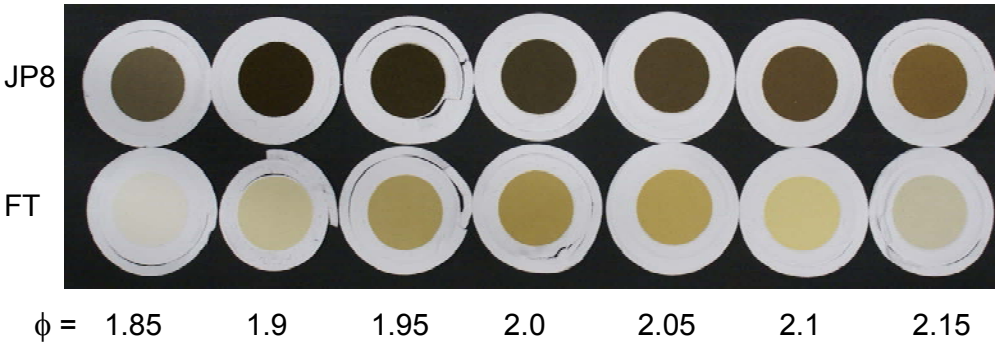

Figure 18. Soot samples on quartz filters for JP8 and FT fuels in the WSR

The particulate matter samples on the quartz filters were also examined to determine the Polycyclic Aromatic Hydrocarbon content (PAH). The PAH content of the soot is of interest because of their role as soot precursors. An ultrasonic solvent extraction process was used to extract the PAH from the soot samples and the PAH concentration expressed as μg of the PAH per volume of gas passed through the samples as determined by GC/FID analysis. The GC/FID compounds quantified were those included in the EPA 610 standard. The concentration results for four of the PAH's examined are shown in Figures 19 through 22. The results show that the PAH levels for the JP8 fuel were much higher at all equivalence ratios than that for the FT fuel. In general, a much larger difference was seen in the ratio of the individual PAH concentrations for the JP vs. the FT fuels than was observed for the ratio of total carbon for the two fuels.

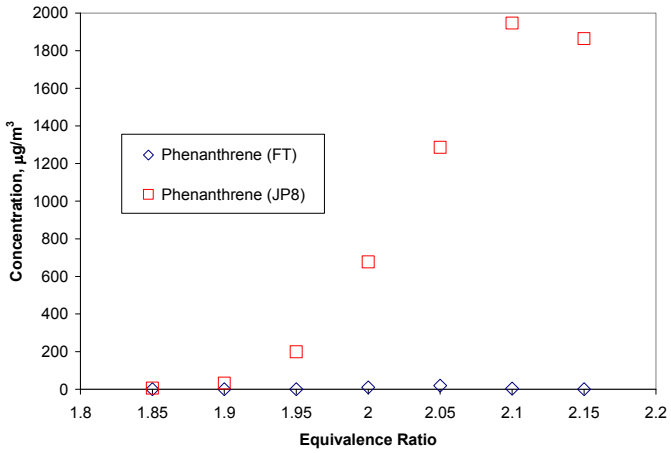

Figure 19. Phenanthrene deposits on filter samples from for JP8 and FT fuels.

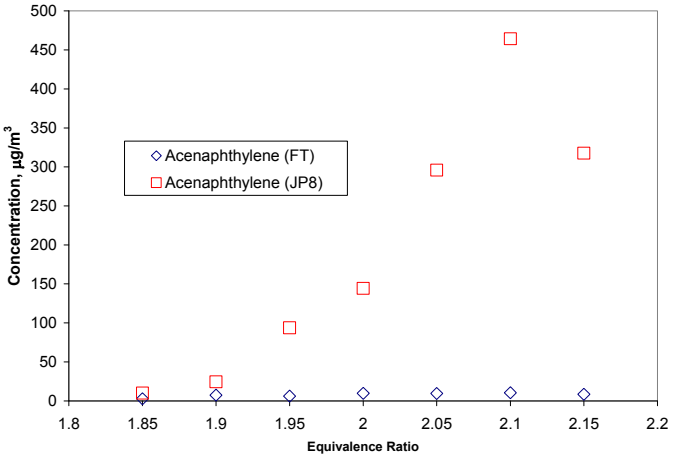

Figure 20. Acenaphtylene deposits on filter samples for JP8 and FT fuels.

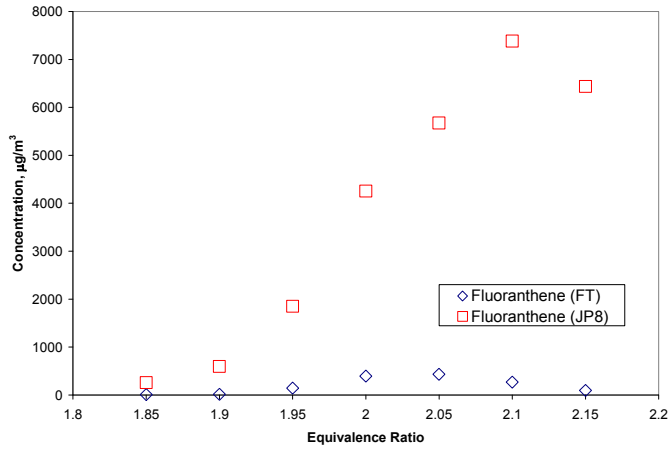

Figure 21. Fluoranthene deposits on filter samples for JP8 and FT fuels.

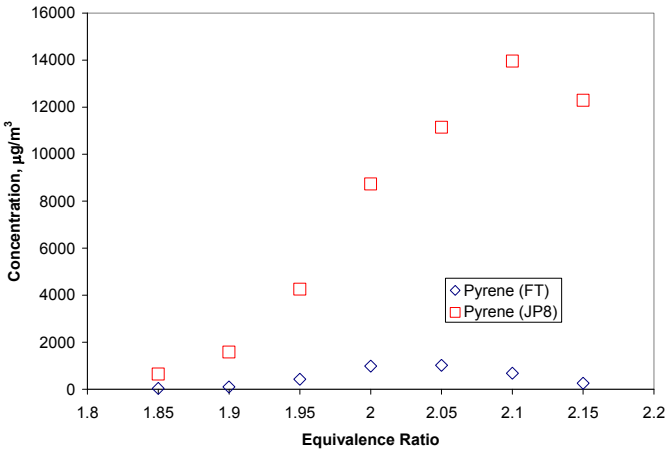

Figure 22. Pyrene Deposits on filter samples for JP8 and FT fuels.

The results shown above show a subset of the experimental results for the rich combustion experiments. It is anticipated that this work will be analyzed and presented at a future conference.

High Pressure WSR Progress

For the high pressure WSR shown, in Figure 23, further progress was made toward assembly. At the rig level, final plumbing of the internal components was finished and various details such as the igniter, and exhaust quench manifolds, and probes have been built and installed. The refractory liner components for the plug flow section of the WSR have been machined and installed in the plug flow section. A mounting stand for the reactor and instrumentation flange has been completed and is in use. The igniter control panel has been designed and has been tested with the igniter. Further preparations on other controls are being made for the facility to accommodate the high pressure WSR.

A major concern for the program has been the vaporizer. During the past year we have successfully and safely vaporized JP8 fuel at pressures up to 5 atm. Because of time constraints, we substituted rich combustion experiments discussed above in place of the high-pressure experiments. High pressure WSR experiments sponsored by AFRL/PRTC are expected to begin in the 2007 Fall.

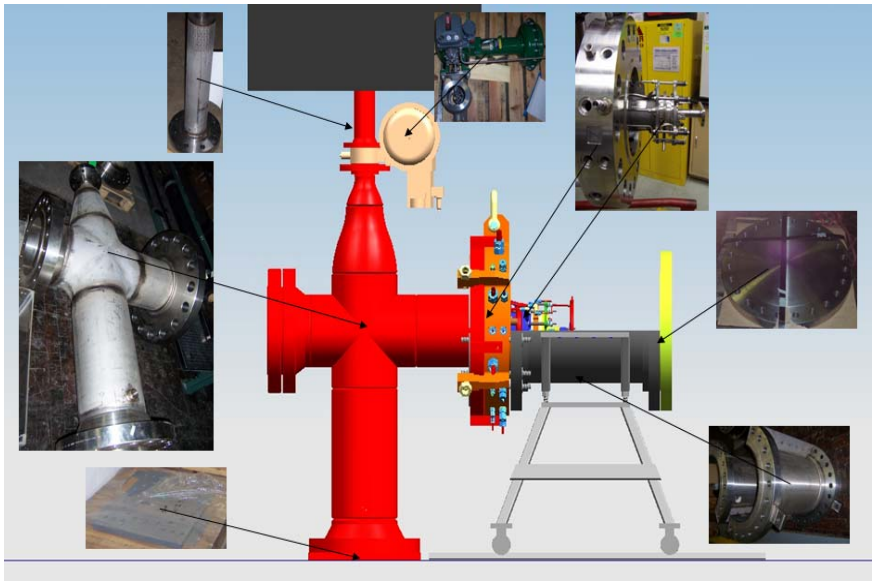

Figure 23. High Pressure WSR test facility

Student Involvement

Mr. Ben Mortimer, a University of Dayton student completed and successfully defended his M Sc. thesis, entitled "Development of an Experimental Technique to quantify the Volatile Composition of Soot Particles Below 200 nm", in November at the University of Dayton. Currently, he is employed at GE Aviation. His thesis focused on determining the apparent volatile fraction of the soot from both the WSR and the exhaust of a T63 gas turbine engine. It was found that the apparent volatile composition of the soot formed in the rich WSR products was much greater than that for the T63. A major question raised as a result of this work is the question of the effect of soot morphology on the apparent size of soot. It is hoped that future morphology studies of samples extracted with a new particle sampler provide insight into these questions. This work was presented at the Dayton Cincinnati Aerospace Symposium in March 2007[3]. In addition two undergraduate students have been involved in the work, one has graduated and has entered graduate school and the other is currently a junior in Mechanical Engineering Department at The University of Dayton.

Summary

We completed work on all the three subtasks and our key conclusions were as follows.

1. The single pulse shock tube was used to study ignition characteristics of a surrogate synthetic fuel, 2-methyl heptane, at three equivalence ratios. The results suggest that activation energy for 2-methyl heptane ignition is significantly lower than that observed for n-heptane ignition.

2. The WSR lean blowout (LBO) data for the JP8 show that the equivalence ratio at blowout varied only about 1% as the loading parameter was doubled. This variation is actually less than the uncertainty of the measurement of the equivalence ratio. The data for the FT fuel show that the equivalence ratio at lean blowout is slightly less than that for the JP8 fuel and shows less than 2.8% increase in equivalence ratio with loading parameter as loading parameter is doubled.

3. Our soot measurements showed that the filters for the JP8 experiments were clearly much darker than those for the FT experiment at the same equivalence ratios, which is in agreement with the quantitative results for carbon mass. In addition, the filters for the FT fuel exhibited a range of colors from light cream though brown which is more indicative of volatile incipient soot as compared to the much blacker more carbonaceous JP8 soot.

4. The soot characterization results show that the PAH levels for the JP8 fuel were much higher at all equivalence ratios than that for the FT fuel. In general, a much larger difference was seen in the ratio of the individual PAH concentrations for the JP vs. the FT fuels than was observed for the ratio of total carbon for the two fuels.

References

1. S. S. Sidhu, J. L. Graham, D. R. Ballal, and H. C. Mongia (2005), “Investigation of Heptane Combustion at 50-atm. Using a Shock Tube,” AIAA Paper No. 2005-1447, to be presented at the 43rd AIAA Aerospace Sciences Meeting, Reno, NV.
2. D. F. Davidson, D. C. Horning, and R. K. Hanson, “Shock Tube Ignition Time Measurements for n-Heptane/O2/Ar and JP-10/O2/Ar Mixtures,” AIAA Paper No. 99-2216 (1999).
3. S. C. Stouffer, D. R. Ballal, J. Zelina, D. T. Shouse, R. D. Hancock, and H. C. Mongia (2005), “Development and Combustion Performance of a High-Pressure WSR and TAPS Combustor,” AIAA Paper No. 2005-1416.
4. Stouffer, S.D., Pawlik, R., Justinger, G., Heyne, J., Zelina, J., Ballal, D. "Combustion Performance and Emissions Characteristics for a Well-Stirred Reactor for Low Volatility Hydrocarbon Fuels", AIAA 2007-5673.
5. Mortimer, B. “Development of an Experimental Technique to Quantify the Volatile Composition of Soot Particles Below 200 nm,” M.Sc. Thesis, Aerospace Engineering Department, The University of Dayton, Dayton, OH November 2006.
6. Mortimer, B. M., Stouffer, S. D., and Dewitt, M.J. "Quantification of the Volatile Composition of the Volatile Composition of Soot Particles Below 200 nm", Presentation at the 32nd Dayton Cincinnati Aerospace Sciences Symposium, March 6, 2007.

Appendix A

Stouffer, S.D., Pawlik, R., Justinger, G., Heyne, J., Zelina, J., Ballal, D. "Combustion Performance and Emissions Characteristics for a Well-Stirred Reactor for Low Volatility Hydrocarbon Fuels", AIAA 2007-5673.

43rd AIAA/ASME/SAE/ASEE Joint Propulsion Conference & Exhibit
8 - 11 July 2007, Cincinnati, OH

AIAA 2007-5663

Combustion Performance and Emissions Characteristics for a Well-Stirred Reactor for Low Volatility Hydrocarbon Fuels

Scott D. Stouffer*
University of Dayton Research Institute, Dayton, OH, 45469

Robert Pawlik†
Air Force Research Laboratory, Wright-Patterson AFB, OH, 45433

Garth Justinger‡, Joshua Heyne§
University of Dayton, Dayton, OH, 45469

Joe Zelina**
Air Force Research Laboratory, Wright-Patterson AFB, OH, 45433

Dilip Ballal††
University of Dayton Research Institute, Dayton, OH, 45469

The performance and gaseous emissions were measured for a well-stirred reactor operating under lean conditions for two fuels: JP8 and a synthetic Fisher-Tropsch fuel over a range of equivalence ratios from 0.6 down to lean blowout. The lean blowout characteristics were determined in LBO experiments at loading parameter values from 0.7 to 1.4. The lean blowout characteristics were then explored under higher loading conditions by simulating higher altitude operation with the use of nitrogen to dilute the air. The results show that the two fuels have very similar combustion performance and lean blowout characteristics. Most of the differences observed in the emissions characteristics can be directly attributed to the difference in the C/H ratio of the two fuels.

Nomenclature

n_{air}	=	Flow rate of air (moles/sec)
EI	=	Emissions Index, g/kg of fuel
FT	=	Fischer-Tropsch Fuel
LHV	=	Lower Heating Value (J/kg)
MW	=	Molecular Weight
R_u	=	Universal Gas constant
slpm	=	Standard Liters Per Minute
UHC	=	Unburned Hydrocarbons

* Senior Research Engineer, Energy and Environmental Engineering Division, Senior Member AIAA.
† Chemist, AFRL/PRTC.
‡ Student, School of Engineering, Mechanical Engineering Department.
§ Student, School of Engineering, Mechanical Engineering Department .
** Senior Research Engineer, AFRL/PRTC, Wright Patterson AFB, AIAA Associate Fellow.
†† Division Head, Energy and Environmental Engineering Division, AIAA Fellow.

V = Reactor Volume
ϕ = Equivalence ratio
ρ = Density (kg/m^3)
τ = Residence time (ms)

I. Introduction

The fundamental understanding of pollutant formation coupled with new technologies will be required to produce cleaner burning, robust combustors and to offset the increased NOx produced by higher combustor inlet pressures and temperatures. To develop advanced combustors in a cost-effective manner by true design-by-analysis approach requires validated unsteady aero design analysis codes that include transient combustion behavior and detailed chemical kinetics. Conventional design practice for combustion systems requires design iterations via expensive component rig testing because current state-of-the-art design codes cannot accurately capture the turbulent-chemistry interaction occurring in the combustor's complex flow environment. Therefore, experimental data from focused smaller-scale experiments to obtain the data for extension of current code capabilities is required.

The Well-Stirred Reactor (WSR) is a versatile laboratory research combustor that simulates the highly turbulent combustion process in a practical gas turbine combustor. The WSR has been used to study high temperature chemical kinetics of gaseous and liquid fuel combustion, combustion stability, lean extinction and blowout limits, and gaseous pollutants (NOx, CO, and unburned hydrocarbons) and particulate emissions in previous studies.[1-5]

Interest in alternative fuels has led to the consideration of the Fischer-Tropsch (FT) process for converting non-conventional hydrocarbon feedstocks into a practical gas turbine fuel. The FT process allows the use of non-conventional hydrocarbons by converting the fuel into synthesis gas (CO and H_2), which can then be converted to hydrocarbon fuel sources. The raw feedstock fuel for the process can be natural gas, coal or other sources. The Department of Defense is currently working with the Department of Energy to develop, test, and certify usage of the FT fuels leading to their use in military and commercial aircraft.[6] The work reported in this paper examines the combustion performance, and emissions characteristics for a well-stirred reactor operating under steady lean combustion for JP8 and a synthetic Fischer-Tropsch jet fuel. Lean blowout limits and gaseous emissions while approaching lean blowout are also examined for the two fuels in the WSR.

II. Experimental Apparatus

The most important characteristic that separates the WSR from other premixed combustion systems is the high rate of continuous mixing of the products and incoming reactants. Ideally, for a "Perfectly-Stirred Reactor" the intense mixing will result in a uniform profile of species and temperature throughout the reactor. However, because of practical limitations on mixing and reaction rates, it is impossible to achieve a perfectly stirred reactor over the entire combustor. For example, in the immediate vicinity of the fuel/air jets there will be a higher fraction of incoming reactants than products of combustion. However, over most of the reactor volume the products and incoming reactants are well mixed. The high degree of mixing with the current design is evident by the high equivalence ratio associated with the soot inception limits and by the temperature profiles across the WSR cross-section measured in previous studies.[3,5]

The 250-ml toroidal WSR, as designed by Nenniger et al.[1] and modified by Zelina[2] and later Stouffer[3], was used for the current experiments. The photo in Fig. 1 shows the WSR rig during operation. A schematic cross section of the reactor and jet ring are shown in Fig. 1(b). The four key parts of the WSR system are: a vaporizer (not shown), the fuel-air injector ring, toroidal WSR combustor, and the plug flow exit section. The two halves of the WSR fit around the jet ring assembly to form the toroidal WSR combustor section. A variety of ceramic and metallic materials have been used for the WSR fabrication in previous studies, and the material used depends

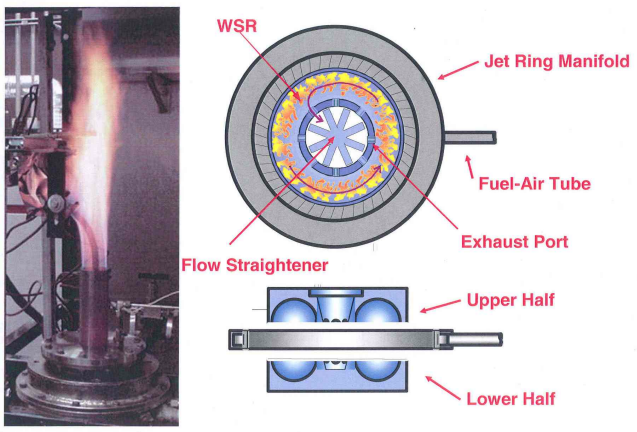

(a) (b)

Figure 1. (a) The Well-Stirred Reactor shown during operation, (b) Cross-section of the WSR.

on the anticipated test conditions. For the current experiment the desire was to operate the combustor under fuel-lean conditions with minimal heat loss through the walls, and so fused-silica ceramic was used for the reactor walls because of its low thermal conductivity, to reduce heat loss, and its low thermal expansion coefficient, which helps to reduce cracking under the fast thermal transients associated with blow out. The Inconel jet ring has 48 fuel/air jets of 0.86 mm diameter that are used to inject the pre-vaporized/premixed reactants at high subsonic or sonic velocity from the outer radius of the toroidal WSR combustor. At low flow rates, the jet ring is cooled by nitrogen impingement to avoid autoignition of the fuel-air mixture within the jet ring manifold. It was found that as the total air flow to the reactor was increased, the need to actively cool the jet ring was reduced. For the experiments, a 6 g/min nitrogen cooling flow rate was used to purge the steel reactor housing. In the reactor, the high velocity reactants continually stir and mix with the combusting gases producing high turbulence and mixing levels in the reacting flow field. The WSR has several access ports for temperature, pressure, and emissions samples, located at the bottom of the WSR. Oil-cooled gas-sampling emissions probes are used for extracting emissions from the reactor. The mixture is then exhausted through eight radial ports at the toroid inner diameter, and turned and straightened before entering the 5-cm diameter plug flow reactor (PFR), where additional measurements can be made.

A facility schematic, shown in Fig. 2, identifies components and instrumentation used for operation of the rig and acquisition of emissions. Air and gaseous fuel flow rates are measured and controlled using thermal mass flow controllers. The uncertainty of the gas flow measurements was +/- 1.5%. The fuel system uses a three-diaphragm pump to continuously supply the fuel mixture to a combination of several pulse dampers and regulators to create a steady pressure source from the pulsing pump. Two parallel control valves, a coarse manual valve and fine adjustment valve are used to control the flow measured by a constant displacement piston flow meter using a PID loop for controlling a fine control valve. The piston flow meter is accurate to within +/- 0.5%, and the estimated overall uncertainty of the liquid flow measurement including calibration was +/-1.4%.

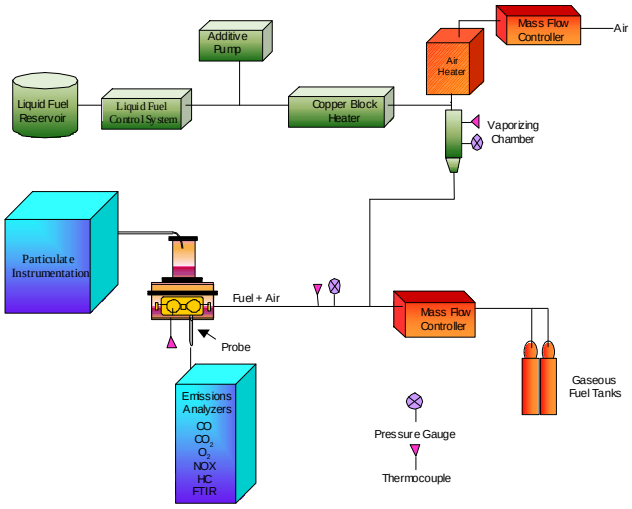

Figure 2. Well Stirred Reactor Air, Fuel and Instrumentation Systems.

PID-controlled electric heaters heat the fuel and air streams entering the reactor. The liquid fuel was sprayed into the vaporizer using an air swirl atomizer nozzle, which uses approximately 10-20% of the total air consumed in the reactor as vaporizer nozzle air to atomize the fuel. The rest of the air (main air) consumed in the reactor was added as a coaxial stream in the vaporizer. The combination of the fuel temperature (~420K), main air temperature (~470-490K), vaporizer nozzle air temperature (~430-460K), and the flow rates were used to control the temperature of the air-fuel mixture entering the reactor. The temperatures of both the fuel and the air were at all times below the known autoignition limits of JP8 fuel. The autoignition limit of the FT fuel was not known but it was assumed that it was between that of JP8 and heptane.

Proper vaporization of all of the lower volatility hydrocarbons is a particular concern for the experiment. The temperature levels of the fuel and air were sufficient to maintain the temperatures of the flow entering the jet ring of the reactor at temperatures above 444K which was above the maximum estimated dew point (404K) of the JP8 mixtures used in the study. As evidence of vaporization it should be noted that the reactor and vaporizer has been used for long duration materials testing experiments which included multiple continuous 12-hr periods of operation on JP8 fuel. During these long-duration experiments, the pressures at the jet ring, and the vaporizer were continuously monitored to assess any potential problems caused by condensation/coking in a filter and check valve located in the line between the vaporizer and the jet ring. The absence of any pressure changes upstream of the reactor at constant flow rates has served as a secondary check for vaporizer effectiveness.

A retractable spark igniter was used to initiate combustion within the reactor. When the reactor is operated on a liquid fuel, it is first started on a gaseous fuel (usually ethylene) and allowed to warm-up to operating temperatures to prevent fuel condensation in the small passages of the jet ring. After allowing the reactor to warm up to operational temperatures, the fuel is smoothly transitioned from a gaseous fuel to a liquid fuel.

Table 1. Properties of the JP8 and FT Fuels

Property	JP8 (3773)	FT (5018)
Molecular Formula	$C_{11.9}H_{22.8}$	$C_{11.9}H_{25.9}$
H/C ratio	1.916	2.165
Stoichiometric Fuel/air	0.0682	0.0666
Molecular Weight	165.9	169.5
Density (g/ml)	0.80	0.755
Heat of Combustion (J/kg)	43276	44135
% Aromatics	17.2	0
Freezing Point (°C)	-51	-51
Flash Point (°C)	45	48

Two fuels; JP8 and S8 Fischer-Tropsch were studied and their properties are shown in Table 1. JP8 is the standard fuel used in U.S. military aircraft. Syntroleum Corporation of Tulsa, OK, produced the S8 fuel from a feedstock of natural gas. However, because the initial step in the fuel manufacturing is to produce synthesis gas, which is then converted to the jet fuel, the properties of the FT fuel considered here are similar to those that would be made by the FT process using other feedstocks, such as coal. The FT fuel is primarily composed of normal and branched alkanes, in contrast to JP8, which can have significant (10-24%) aromatic content. As shown in Table 1 many of the properties of the S8 are similar to those for JP8. A noted disadvantage of the FT fuel is the lower density, which is partially offset by its increased heat of combustion. Further investigations of the properties and of FT and JP8 fuels are discussed in Refs. 6-9.

A. Instrumentation

The reactor temperature was measured by a bare wire type B thermocouple (0.2 mm diameter) which was placed at a distance of 4.8 mm up from the bottom of the toroidal reactor section. The radial position of the thermocouple in the toroid corresponds to the position of 50% of the cross-sectional area of toroid. Facility operation was monitored using thermocouples in the air lines, WSR jet ring, inlet, reactor, housing, and stack. The pressure rise in the reactor was determined using an absolute pressure transducer.

The gaseous emissions were sampled from an oil-cooled probe placed at an equivalent position from the emissions sampling probe, which was located 90 degrees around the major axis of the torrid and at the same height (4.8 mm) from the bottom of the reactor as the thermocouple. The outer diameter of the cooled probe was 9.5 mm. The probe was constructed of stainless steel and had an inner tube with a diameter of 1.27 mm that was used to extract emission gases and was surrounded by two concentric tubes that formed a cooling jacket around the probe. A circulating oil heater is used to cool the emissions probes to a temperature of 420 K. Electrically heated sampling lines, maintained at above 150°C, were used to transport samples to the emissions instrumentation.

Gaseous emissions analyzers were used for on-line measurement of CO, CO_2, NO_x, O_2, and unburned hydrocarbons within the reactor and water and minor species were measured by the use of a multigas FTIR. A sketch of the sample train is shown in Fig. 3. Flow from the probe was sent to either the FTIR or the rest of the analyzers shown on the right side of Fig. 3. With the setup it was possible to sample to either the FTIR or the other analyzers, but not to both sets of instruments simultaneously. Each of the analyzer trains had a filter in series with it for protection from particulate matter. The volume associated with the filters caused a lag in the time response of the analyzers.

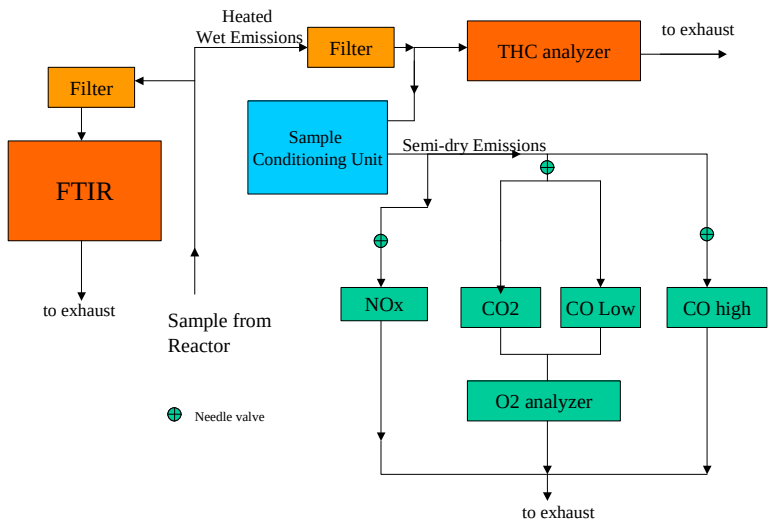

Figure 3. Sample Train for Gaseous Emissions Measurements.

The FTIR system used an MKS 2030 with a 5.11-m long gas cell path length. The analyzer is heated and allows online detection of major gaseous species along with subsequent detailed investigation of the spectra saved. It is capable of measuring species of CO, CO_2, H_2O, NO, NO_2, and other compounds that absorb infrared radiation. Flow to the FTIR was limited to 1-2 lpm. At the lowest reactor flow rates (lowest reactor pressures) an

ejector mounted on the exhaust side of the FTIR was used to pull gas through the analyzer. This typically lowered the pressure in the analyzer by less than 0.02 atm. At higher reactor flow rates the pressure in the reactor was sufficient to push the gas though the analyzer. Uncertainty for the FTIR measurements was typically +/- 3%.

The emissions train for the rest of the instruments is shown on the right side of Fig. 3. The unburned hydrocarbons were measured using a heated Flame Ionization Detector (FID) analyzer (VIG model 600), which measures the unburned hydrocarbons on a wet basis. The analyzer had adjustable ranges of 100 to 100000 ppm propane. The rest of the sample stream was routed to a sample conditioning unit, which consists of a pump and a chiller-based sample dryer that dried the sample to a dew point of roughly 5°C before allowing the semidry sample to flow to the other analyzers, which were arranged in a parallel-series arrangement. The CO_2 and CO were measured by a three-cell non-dispersive infrared analyzer (California Analytical model 600). There are two CO cells, a low concentration cell, which has a maximum range of 3000 ppm, and a high CO that was set at a range of 2%. A paramagnetic analyzer (Horiba MPA) was used to measure the oxygen. Repeatability for the gas analyzers was within +/-1% over the course of a day and the calibration gases used to set the span of the analyzers were certified to +/- 2%.

The response time of the analyzers to a fast transient such as a lean blowout was an issue during the study. The requirement to continuously pass the emissions through sample volumes associated with the filters and sample-conditioning units slows the time response of the system. Another consequence of the finite time response of the sample system components is that the time response of the each of the analyzers may be different. Because of the finite volumes associated with system the measurement from an analyzer is a running time average of the emissions produced in the combustor, which is not an issue for the characterization of steady operation, but it presents limitations on capturing fast transients. Fig. 4 shows the response of the sample train to a typical blowout. The blowout event (at time = 0 s) is marked by a steep decrease in the temperature in the reactor. The UHC analyzer was the first to respond to the blowout, which is expected because of its faster response time (5 seconds), shorter length to the source, and smaller system volume. The rest of the analyzers have slower response times and have the added system volume associated with the filters and the sample-conditioning unit, resulting in a slower overall response. The response of the FTIR analyzer (not shown) was typically within 16-24 seconds of an event in the reactor. The results reported as blowout conditions from the sample train are those that occur at the time of blowout as indicated by the reactor temperatures.

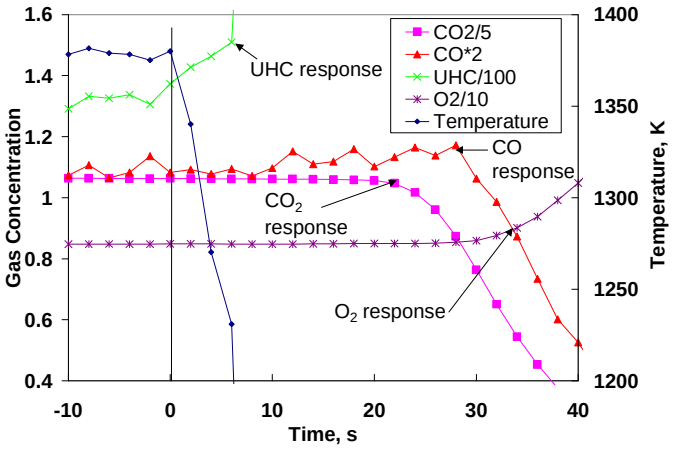

Figure 4. Time Response of the Emissions Analyzers During a Typical Lean Blowout.

B. Experimental conditions

During the experiments, the reactor was operated under a range of air flow rates from 300-600 g/min (250 to 500 slpm). The fuel/air mixture entering the jet ring was held to a constant temperature of 444 +/-6 K, and the pressure ratio across the injector ring nozzles was greater than 2, implying from one-dimensional compressible flow theory that the flow across the nozzles was choked and that the fuel/air mixture entering the WSR was sonic. The fuel flow was varied to obtain the desired equivalence ratio for the two fuels. All of the penetration paths to the reactor are sealed allowing the reactor to maintain a pressure slightly (1-3 kPa) above ambient pressure.

For the emissions measurements the air and fuel flows were established at the levels required and the reactor temperature was allowed to level out before taking emissions data. Emissions data were taken for a fixed experimental condition using both the FTIR and the other analyzers in sequence.

The lean blowout tests were conducted by gradually reducing the fuel equivalence ratio at fixed air flow rates until the flammability limit was reached in the reactor. A lean blowout was noted to correspond to an immediate drop in temperature of the reactor and usually coincided with a sharp change in the noise generated by the reactor. After the lean blowout in the reactor the fuel flow was diverted from the vaporizer, the reactor was then re-lit using

lower liquid fuel and air flow rates. Typically two to four separate LBO events were measured for each fuel at a given air flow rate.

III. Experimental Results

The experimental results for combustion performance and emissions that will be presented were determined for two constant air flow rates 300 g/min and 600 g/min.

The average residence time, τ, is defined by the following equation:

$$\tau \equiv \frac{\rho V}{\dot{m}}, \tag{1}$$

Where V is the reactor volume, m is the mass flow and the density, ρ, is calculated by the ideal gas law,

$$\rho = \frac{P(MW)}{R_u T}, \tag{2}$$

The pressure and the temperature were measured during the experiments and the molecular weight of the products was estimated from equilibrium values. For the range of lean combustion conditions explored in this study, the changes in the molecular weight and reactor pressure are small, so that the variations in the residence time are principally caused by changes in the reactor temperature and mass flow. At the highest air flow rates studied (600 g/min) the residence time ranged from 6.3 ms near lean blowout to 5 ms at $\phi = 0.6$, while the residence time was approximately twice as much for the lowest air flow rates (300 g/min) studied. For the plots shown below blue is used to indicate the results for the FT fuel and red for the JP8 fuel. Also, squares are used to indicate the lower flow rate (higher residence time) and the triangles are used to show the results for the higher mass flows (lower residence times).

One of the primary measures of combustor performance in the WSR is the temperature in the combustor. Figure 5 shows the temperatures in the WSR. As expected, the temperature increased with the increases in equivalence ratio. The temperatures show close agreement for both fuels at the two flow rates. For equivalence ratios at or above 0.45, the reactor was operated at point for long periods of time and multiple 30-second averages of temperature and emissions were measured using both sample trains. At equivalence ratios less than 0.45 the reactor equivalence ratio was gradually lowered toward lean blow out and the data points shown also represent 30-second averages. But, for the points below $\phi = 0.45$ the reactor was not held at the same condition for as long, and it is thought that the non-equilibrium between the gas temperature and the wall temperature, as the reactor was cooling down, may be responsible for the small scatter in the WSR temperature data at the lower equivalence ratios.

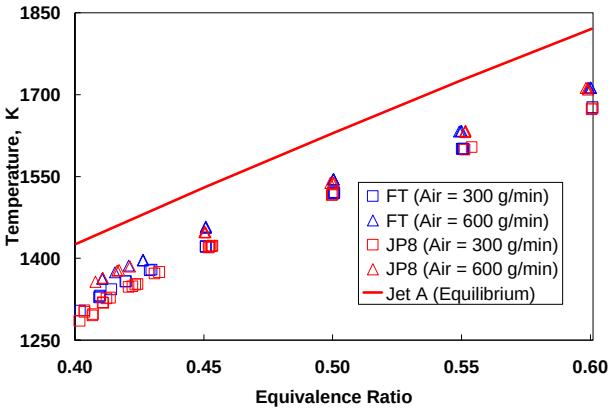

Figure 5. Temperatures Measured in the WSR.

The temperature results are also compared to equilibrium calculations of the adiabatic flame temperature from the NASA Chemical Equilibrium Code.[10] The difference between the experimental temperatures and the calculated adiabatic flame temperature were highest for the lower flow rate conditions implying that the effect of heat loss was less for the higher flow rate cases.

The measured O_2 and CO_2 data are shown plotted along with the equilibrium values for JP8 and the ideal concentration for the FT fuel in Figs. 6 and 7, respectively. The overall results show the expected increased oxygen consumption and CO_2 production as the equivalence ratio is increased. It was found that with both of the fuels the CO_2 production was higher and the O_2 consumption was higher at the higher mass flow cases. This result is also consistent with trends of temperature vs. mass flow observed in Fig. 5. The CO_2 observed for the JP8 was higher than that for the FT fuel, which was expected based on the higher carbon fraction for the JP8 fuel. For ϕ>0.5 the

ratio of the CO_2 produced for the JP8 to that for the FT ranged from 1.033-1.044, while the ideal ratio of the CO_2 produced under complete oxidation to CO_2 and H_2O for the two fuels was 1.044. For the higher equivalence ratios shown the results parallel the ideal limits, but as lean blowout was approached the oxygen consumption and CO_2 production depart further from the ideal limits. The departure from the ideal as lean blowout is approached is also consistent with the temperature trends shown above; as less CO_2 is formed the combustion temperatures decrease.

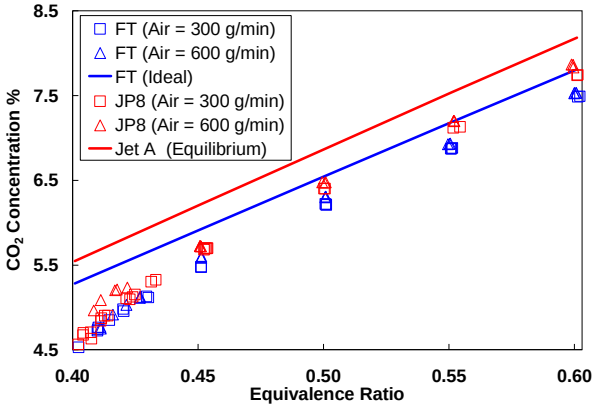

Figure 6. CO_2 Concentration Measured in the WSR.

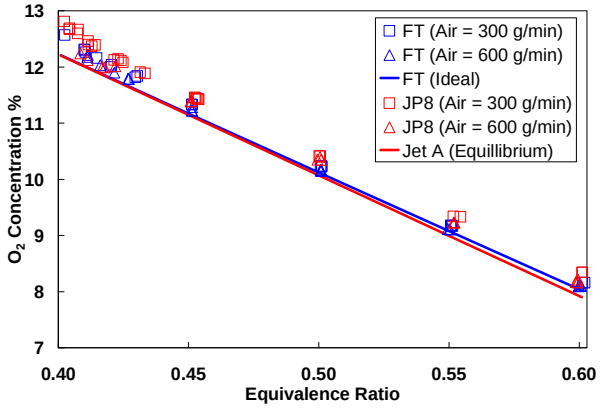

Figure 7. Oxygen Concentration Measured in the WSR.

The water produced in the WSR was measured by the FTIR. The results are shown in Fig. 8 along with an equilibrium and ideal calculation for the water in the exhaust based on complete conversion of the fuel to CO_2 and H_2O. The results show the expected increase in H_2O concentration with equivalence ratio and show good agreement with the equilibrium and ideal water concentrations. The H_2O levels were higher for the FT fuel cases across all of the equivalence ratios studied. Because of the higher H/C ratio of the FT fuel, it was expected that the H_2O concentration in the exhaust would be higher for the FT than that for the JP8 fuel. A comparison of the experimental values in the range from ϕ = 0.45 to 0.6 showed that the ratio of the water concentration for the FT exhaust to that of the JP8 was 1.07-1.09, which brackets the value of the ideal ratio (1.08) of the water produced for complete combustion of the two fuels. As the equivalence ratio was lowered toward lean blowout the water production in the reactor was shown to drop as it did for the CO_2.

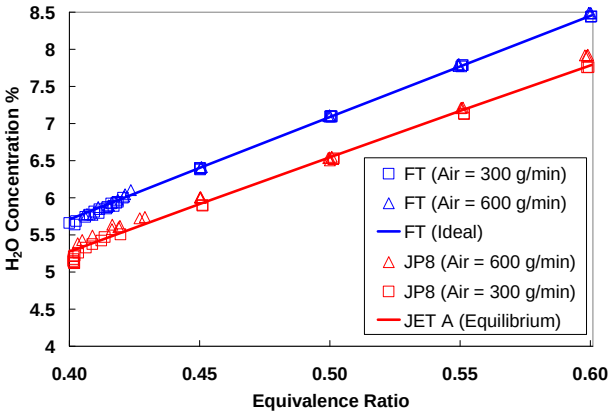

Figure 8. Water Concentration Measured in the WSR.

The unburned hydrocarbons (UHC) measured in the WSR are shown in Fig. 9 expressed as an emissions index. Above ϕ = 0.45 the UHC level was low and the UHC level increased dramatically as ϕ was decreased below ϕ = 0.45. The results are plotted vs. temperature to emphasize the effect of reactor temperature on the unburned hydrocarbon level. It can be seen that in the region leading up to lean blowout that UHC production is more dependant on reactor temperature than the residence time or fuel type.

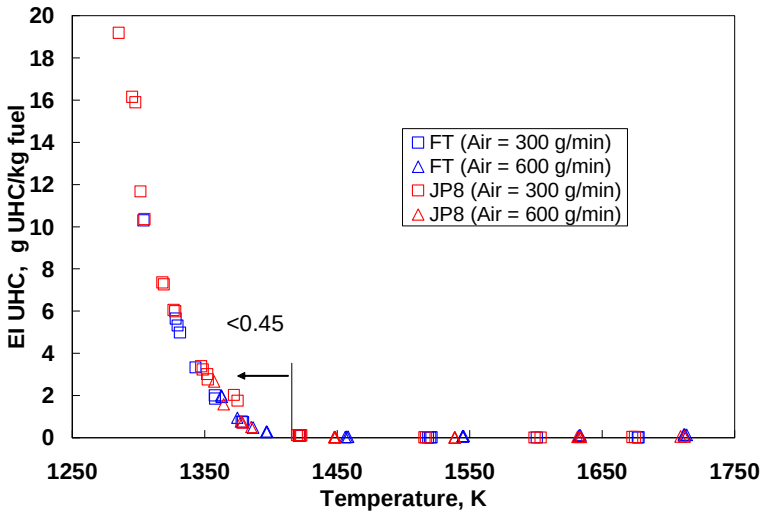

Figure 9. Emissions Index of Unburned Hydrocarbons.

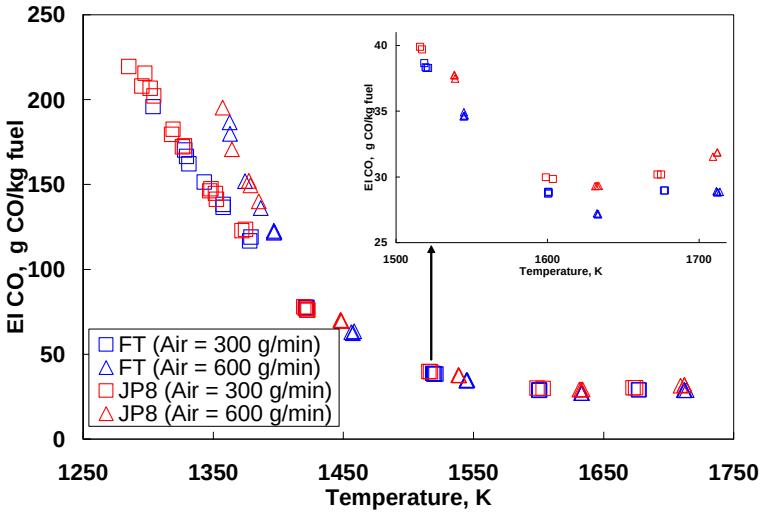

Figure 10. Emissions Index of Carbon Monoxide.

The carbon monoxide emissions are shown in Fig. 10 plotted vs. temperature. The results show that for temperatures above 1400 K (ϕ>0.45) the CO is dependant of the temperature and is almost independent of the residence time for the flow rates considered. Also, in this region the CO levels in this region are slightly higher for the JP8 cases. The CO is shown to decrease to a minimum at approximately 1630 K and then gradually increases as temperature is increased. This existence of a minimum CO value has been seen previously for other fuels.[2,4] As the temperature is increased further more CO is formed as a result of CO_2 dissociation. As the temperature is lowered below 1630 K the CO increases due to quenching of the reactions before CO_2 can be formed, resulting in higher CO levels. As lean blowout is approached for temperatures below 1400 K there is an effect of the residence time on the CO production, with lower residence times (higher mass flows) leading to higher CO values than the higher residence time cases. Note that in this region, for the same temperature and residence time, the CO levels are approximately equal for the two fuel types.

The combustion efficiency was calculated from the SAE Aerospace recommended Practice ARP 1533[11] using measurements of CO and UHC:

$$\eta_C = 1 - 10109 \frac{EI_{CO}}{LHV} - \frac{EI_{UHC}}{1000} \tag{3}$$

where: EI is emissions index and LHV is the lower heating value of the fuel.

The results show that the combustion efficiency is almost identical for the two fuels. For equivalence ratio values above ϕ = 0.5 the combustion efficiency was higher than 99% for both of the fuels. The major portion of the combustion inefficiency is due to the production of CO rather that the production of UHC, and so the efficiency results strongly resemble a mirror image of the plot for the CO vs. temperature in Fig. 10. As the lean blowout is approached at the lower equivalence ratios the combustion efficiency drops dramatically. The efficiency decrease with temperature drop is more pronounced for the shorter residence time cases.

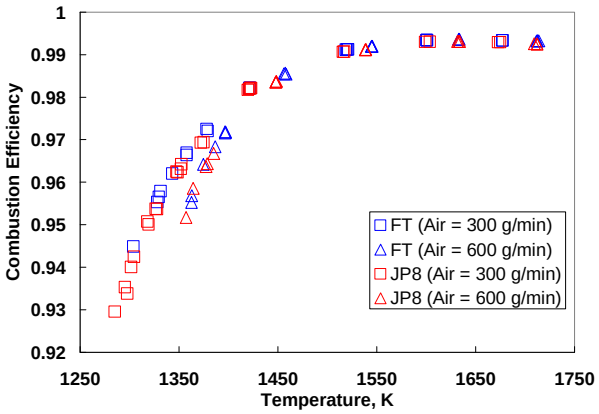

Figure 11. Combustion Efficiency vs. Temperature in the WSR.

All of the data shown above was obtained under quasi-steady conditions. The response of the reactor to the lean blowout will now be examined. In general as lean blowout was approached the temperature began to drop and the hydrocarbons and carbon monoxide increased. As the reactor cooled, the combustion efficiency decreased resulting in less heat release and further production of CO and UHC. Eventually there is not enough energy released in the reactor to sustain combustion and the flammability limit is reached.

Figure 12 shows the lean blowout data expressed as equivalence ratio at LBO vs. Loading parameter where the loading parameter is determined from:[12]

$$LP = \frac{n_{air}}{VP^{1.75}} \qquad (4)$$

where: n_{air} = flow rate of air in moles/sec
V= volume of the reactor in liters
P = pressure in the reactor in atm

The LBO data for the JP8 show that the equivalence ratio at blowout varied only about 1% as the LP was doubled. This variation is actually less than the uncertainty of the measurement of the equivalence ratio. The data for the FT fuel show that the equivalence ratio at lean blowout is slightly less than that for the JP8 fuel and shows less than 2.8% increase in equivalence ratio with loading parameter as loading parameter is doubled.

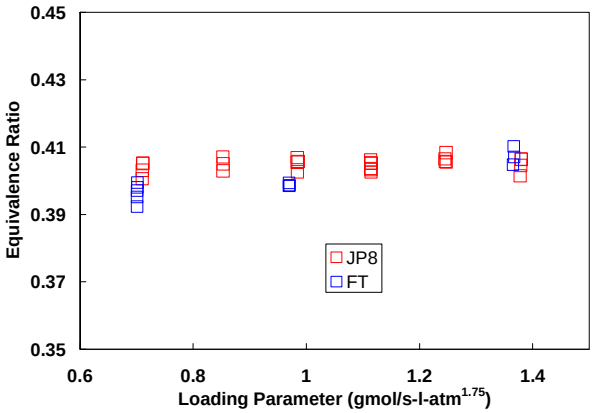

Figure 12. Equivalence Ratio at Lean Blowout vs. Air Loading Parameter.

Figure 13 shows that the temperature at lean blowout increased as the loading parameter increased. Note that the higher loading parameter cases correspond to lower residence times in the reactor and thus less time for reactions to complete, therefore higher temperatures are required to maintain the reaction rates. The temperatures at blowout for the two fuels are very similar.

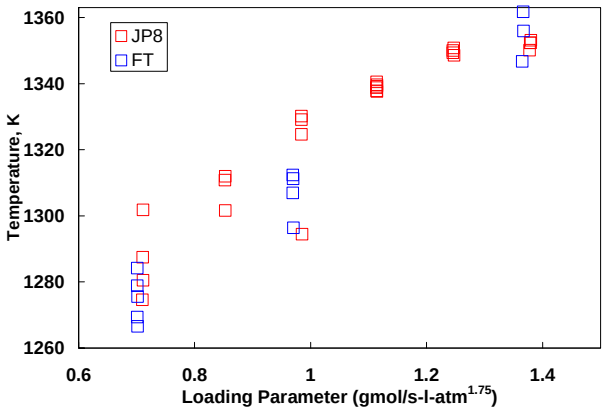

Figure 13. Temperatures Measured in the WSR at Lean Blowout.

While the equivalence ratio and temperatures at lean blow out was well defined and very repeatable, it was found that the emissions varied for a given blowout condition. The carbon monoxide and total hydrocarbon levels at lean blowout are shown in Figs. 14 and 15, respectively. The CO levels at blowout are relatively flat but scattered within a +/-16% band. In contrast, the results for unburned hydrocarbons show a decreasing trend of UHC with loading parameter. Note that the condition of higher loading also corresponds to higher mass flows, and as shown in Fig. 13, the temperature in the reactor at LBO increases with higher temperatures.

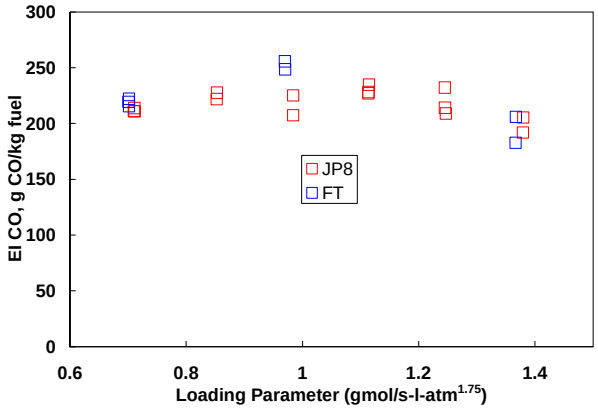

Figure 14. Emissions Index of Carbon Monoxide Measured at LBO.

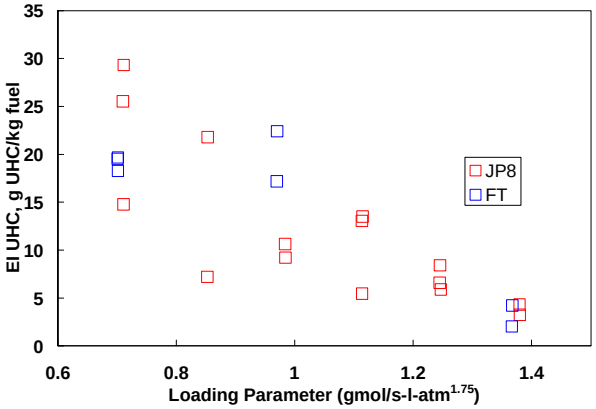

Figure 15. Emissions Index of Unburned Hydrocarbon Level Measured at LBO.

Details of the chemical constituents of the UHC were determined by FTIR analysis and it was found that ethylene, formaldehyde, and acetylene were found to be present in the exhaust at conditions near lean blowout and not found in significant quantities at temperatures above 1450 K. The results are shown in Figs. 16 and 17 where ethylene, formaldehyde, and acetylene are plotted along with temperature vs. time for the two flow rates. The data for all of the conditions show that as the temperature decreased on the approach to blow out the concentrations of the individual hydrocarbons all increased. Close examination of the plots shows the sensitivity of the individual hydrocarbon concentrations to the fluctuations of the temperatures, as changes in the temperature are followed by changes in the opposite direction by the hydrocarbon concentrations. As the flowrate increased, the unburned hydrocarbons dropped for both of the fuels, this observed trend is in agreement with the trends shown for all of the UHC's shown in Fig. 15. For the cases shown here, the levels of the ethylene and the formaldehyde at blowout were slightly higher for the FT fuel, however, it should be noted that the temperature levels at blowout for the FT fuels shown here are lower than those for the JP8.

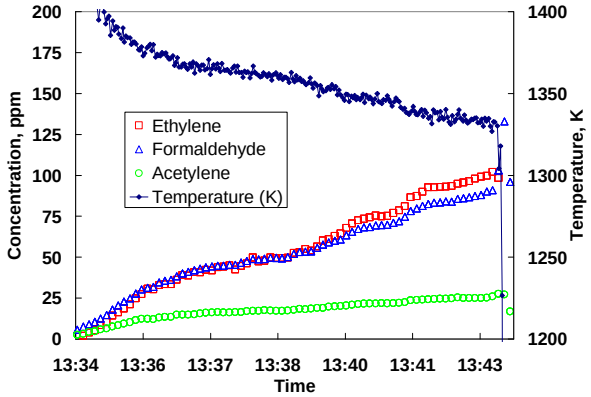

(a)

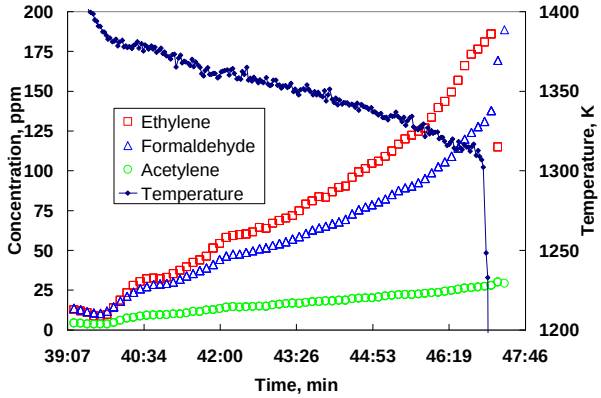

(b)

Figure 16. Ethylene, Acetylene, and Formaldehyde Formation as LBO is Approached for Total Air Flow of 420 g/min (a) JP8, (b) FT.

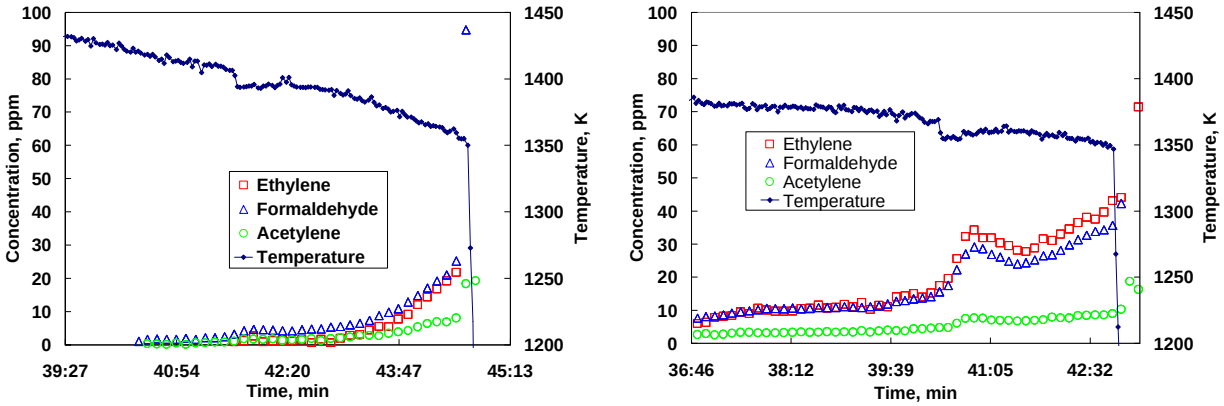

Figure 17. Ethylene, Acetylene, and Formaldehyde Formation as LBO is Approached for Total Air flow of 600 g/min (a) JP8, (b) FT.

The lean blowout at higher reactor loading was explored using the method outlined by Sturgess[13] to simulate high altitude (lower pressures) by nitrogen dilution of the air stream in the reactor. The combined volume flow rate of nitrogen and air was maintained at a constant value and the mole fraction of the oxygen in the air and nitrogen was adjusting the N_2/Air balance. The results shown in Fig. 18 show an increase of equivalence ratio at LBO as the oxygen content of the air decreased. Similar to the results for the lower combustor loading cases, the equivalence ratio at LBO was almost identical for the two fuels under the higher combustor loading conditions shown in Fig. 18. It is possible to estimate the effective altitude and assign a loading parameter by the procedure outlined in Ref. 13; however, this analysis will be performed at a later time.

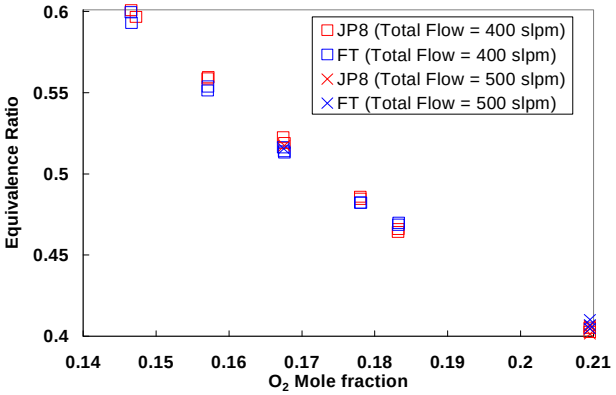

Figure 18. Equivalence Ratio at Lean Blow Out vs. Oxygen Fraction in Air Stream.

IV. Summary and Conclusions

The performance and gaseous emissions were measured for a well-stirred reactor operating under lean conditions for two fuels: JP8 and a synthetic Fisher-Tropsch fuel over a range of equivalence ratios from 0.6 down to the lean blowout. The lean blowout characteristics were determined in LBO experiments at loading parameter values from 0.7 to 1.4. The lean blowout characteristics were then explored under higher loading conditions by simulating higher altitude operation with the use of nitrogen as a dilution gas for the air stream. The experiments showed that:

1. The lean blowout characteristics for the two fuels were close under both low loading and high loading conditions.
2. The combustion temperatures and observed combustion efficiencies were similar for the two fuels.
3. The gaseous emissions were similar for the two fuels and the differences in the H_2O and CO_2 emissions appear to be directly relatable to the C/H ratio for the fuels.

Acknowledgments

The authors are grateful for the help of Mr. Mike Arstingstall of UDRI for technical support on the construction of the WSR and associated systems. The efforts of Mr. Edward Strader of UDRI on the instrumentation and Mr.

Tom McCray of ISSI for data acquisition support are also gratefully acknowledged. This work was funded by GE Aviation subcontract No. 200-18-14U38773, under a NASA prime award no. NAS3-01135 with Dr. Timothy J. Held serving as the contract monitor.

References

[1]Nenniger, J. E., Kridiotis, A., Chomiak, J., Longwell, J. P., and Sarofim, A. F., "Characterization of a Toroidal Well Stirred Reactor," *Twentieth Symposium (International) on Combustion*, The Combustion Institute, pp. 473-479, 1984.

[2]Zelina, J., "Combustion Studies in a Well-Stirred Reactor," Ph.D. Thesis, University of Dayton, Dayton, OH, 1995.

[3]Stouffer, S. D., Striebich, R. C., Frayne, C. W., and Zelina, J., "Combustion Particulates Mitigation Investigation Using a Well-Stirred Reactor," AIAA Paper No. 2002-3723, 2002.

[4]Blust, J.W., Ballal D.R., Sturgess, G.J., "Fuel effects on the Lean Blowout and Emissions from a Well-Stirred Reactor," *Journal of Propulsion and Power*, Volume 15, Number 2. pp. 216-223, 1999.

[5] Stouffer, S. D., Ballal, D. R., Zelina, J., Shouse, D. T., Hancock, R. D., and Mongia, H. C.' "Development and Combustion Performance of a High Pressure WSR and TAPS Combustor," AIAA Paper 2005-1416, 2005.

[6]Harrison, W.E., and Zabarnick, S., "The OSD Assured Fuels Initiative-Military Fuels Produced from Coal," Proceedings of 31st International Technical Conference on Coal Utilization and Fuel Systems, 2006.

[7]Dewitt, M.J, Striebich, R.C., Shafer, L., Zabarnick, S, Harrison, W.E, Minus, D.E., Edwards, T., "Evaluation of Fuel Produced by the Fischer-Tropsch Process for Aviation Applications," Preprints of the AIChE, 2007.

[8]Edwards, T, Minus, D.E., Harrison, W.E., Corporan, E., DeWitt, M.J., Zabarnick, S., and Balster, L., "Fischer-Tropsch Jet Fuels-Characterization for Advanced Aerospace Applications," AIAA 2004-3885, 2004.

[9]Shafer, L.M., Striebich, R.C., Gomach, J., and Edwards, T, "Chemical Class Composition of Jet Fuels and Other Specialty Kerosene Fuels," AIAA 2006-7972, 2006.

[10]Gordon, S., and McBride, B., "Computer Program for Complex Chemical Equilibrium Compositions and Applications," NASA Reference Publication 1311, October, 1994.

[11]Aerospace Recommended Practice 1533, "Procedure for the Calculation of Gaseous Emissions from Aircraft Turbine Engines," Society of Automotive Engineers, Inc., Warrendale, PA, pp. 1-36, 1994.

[12]Lefebvre, A.H., *Gas Turbine Combustion*, Hemisphere Publishing Corp., McGraw-Hill, NY, 1983.

[13]Sturgess, G.J., Heneghan, S.P., Vangsness, M.D., Ballal, D.R., Lesmerises, A.L. "Lean Blowout in a Research Combustor at Simulated Low Pressures," *ASME Journal of Engineering for Gas Turbines and Power*, Volume 118, pp. 145-153, 1996.

REPORT DOCUMENTATION PAGE	Form Approved OMB No. 0704-0188

1. REPORT DATE *(DD-MM-YYYY)*	2. REPORT TYPE	3. DATES COVERED *(From - To)*
01-06-2008	Final Contractor Report	

4. TITLE AND SUBTITLE
Intelligent Engine Systems
Alternate Fuels Evaluation

5a. CONTRACT NUMBER
NAS3-01135

5b. GRANT NUMBER

5c. PROGRAM ELEMENT NUMBER
5

6. AUTHOR(S)
Ballal, Dilip

5d. PROJECT NUMBER

5e. TASK NUMBER
37

5f. WORK UNIT NUMBER
WBS 984754.02.07.03.11.03

7. PERFORMING ORGANIZATION NAME(S) AND ADDRESS(ES)
The University of Dayton
300 College Park
Dayton, Ohio 45469

8. PERFORMING ORGANIZATION REPORT NUMBER
E-16496

9. SPONSORING/MONITORING AGENCY NAME(S) AND ADDRESS(ES)
National Aeronautics and Space Administration
Washington, DC 20546-0001

10. SPONSORING/MONITORS ACRONYM(S)
NASA

11. SPONSORING/MONITORING REPORT NUMBER
NASA/CR-2008-215237

12. DISTRIBUTION/AVAILABILITY STATEMENT
Unclassified-Unlimited
Subject Category: 07
Available electronically at http://gltrs.grc.nasa.gov
This publication is available from the NASA Center for AeroSpace Information, 301-621-0390

13. SUPPLEMENTARY NOTES

14. ABSTRACT
The performance and gaseous emissions were measured for a well-stirred reactor operating under lean conditions for two fuels: JP8 and a synthetic Fisher-Tropsch fuel over a range of equivalence ratios from 0.6 down to the lean blowout. The lean blowout characteristics were determined in LBO experiments at loading parameter values from 0.7 to 1.4. The lean blowout characteristics were then explored under higher loading conditions by simulating higher altitude operation with the use of nitrogen as a dilution gas for the air stream. The experiments showed that: (1) The lean blowout characteristics for the two fuels were close under both low loading and high loading conditions. (2) The combustion temperatures and observed combustion efficiencies were similar for the two fuels. (3) The gaseous emissions were similar for the two fuels and the differences in the H_2O and CO_2 emissions appear to be directly relatable to the C/H ratio for the fuels.

15. SUBJECT TERMS
Gas turbine engines; Fuel systems; Emissions

16. SECURITY CLASSIFICATION OF:			17. LIMITATION OF ABSTRACT	18. NUMBER OF PAGES	19a. NAME OF RESPONSIBLE PERSON
a. REPORT	b. ABSTRACT	c. THIS PAGE			STI Help Desk (email:help@sti.nasa.gov)
U	U	U	UU	39	19b. TELEPHONE NUMBER *(include area code)* 301-621-0390